

THESIS

**ANAEROBIC DIGESTION COMPARISON OF MANURE LEACHATE BY HIGH-RATE
ANAEROBIC REACTORS**

Submitted by

Carlos Enrique Quiroz Arita

Department of Civil and Environmental Engineering

In partial fulfillment of the requirements

For the Degree of Master of Science

Colorado State University

Fort Collins, Colorado

Fall 2013

Master's Committee:

Advisor: Sybil Sharvelle

Kenneth Carlson
Jessica Davis

ABSTRACT

ANAEROBIC DIGESTION COMPARISON OF MANURE LEACHATE BY HIGH-RATE ANAEROBIC REACTORS

A multi-stage anaerobic digester (MSAD) has been developed to obtain high organic leachate from high solids organic waste, thus high-rate anaerobic reactors can be fed by manure leachate, which can be obtained from a leachate bed reactor. Such configuration not only makes feasible the application of high-rate reactors to treat high solids content manure, but also the hydrolysis and the methanogenesis stages can be separated and controlled, individually. However, limited research is available on achieving ideal hydrodynamic conditions, inoculation, and performance of high-rate anaerobic reactors when manure leachate is used as the carbon source. Thus, this research is aimed not only to compare the performance of three different reactor configurations; the Upflow Anaerobic Sludge Blanket (UASB), fixed film, and a hybrid for processing manure leachate as a carbon source, but also to establish design criteria for such reactors including organic loading rates (OLRs) and hydraulic loading rates (HLRs).

In the first part of this research, the influence of the hydraulic loading rates (HLR) in high-rate anaerobic reactors was investigated. The upflow anaerobic sludge blanket (UASB) reactor depicted a Morrill dispersion index (MDI) of 1.7, which is measured to evaluate the plug flow conditions of a reactor by approaching a value of 2 or less, at a HLR of $0.296 \text{ m}^3/\text{m}^2\text{-h}$. On the other hand, a MDI of 4 was observed when the HLR was increased to $0.829 \text{ m}^3/\text{m}^2\text{-h}$. The variation of the HLR had not notable impact MDI of the fixed-film and hybrid reactors; however,

short circuits were observed at low HLR. Thus, the most suitable HLRs of such reactors were $10.632 \text{ m}^3/\text{m}^2\text{-h}$ for the fixed-film reactor and $12.450 \text{ m}^3/\text{m}^2\text{-h}$ for the hybrid reactor.

To evaluate the performance of the UASB, fixed-film, and hybrid reactors to treat manure leachate, this research resulted in development of a method to inoculate such reactors in a single inoculation reactor. The accomplishment of the inoculation was measured by the redox potential, with values below -300 mV after seven days and remained steady until the day 33 with methane percentages in biogas ranging from 45% to 83%. Additionally, plastic media from the inoculation reactor was tested by the biochemical methane potential (BMP) assay, where inoculated organisms were confirmed to produce methane when supplied with glucose as a substrate. In spite that a hybrid anaerobic reactor inoculated with biomass obtained from an UASB reactor, plastic media, and manure leachate was successfully operated at an OLR of $4 \text{ kg/m}^3\text{-d}$, when transferring the inoculated sludge and media to high-rate reactors, anaerobic digestion was not accomplished. The experiment setup did not support maintenance of anaerobic conditions. In addition, manifolds and open-channel flows were recommended in this research to enhance the reactors configurations. Moreover, results from hydrodynamic studies were applied to provide recommendations for future design parameter, which are included in this thesis.

ACKNOWLEDGEMENTS

I would like to express my deep gratitude to my advisor, Dr. Sybil Sharvelle, for her support throughout this research work. I would also like to express my appreciation to Dr. Kenneth Carlson for his wisely guidance at this stage of my life. I wish to thank Dr. Jessica Davis for her willingness to find always a time to give her assistance.

I would also like to extend my thanks to Dr. Karan Venayagamoorthy for his important contributions to my research and Julio A. Zimbron for providing his helpful insights. My grateful thanks are also extended to my fellow student Patrick Brice, who was always willing to give me a hand when I needed. I would like to thank Mitchell Olson, Paige Griffin , and Lucas Loetscher for their patience and technical contributions to my thesis.

My special thanks are extended to my sponsor, Fulbright LASPAU, and its whole staff for such a great opportunity. Also, I thank Christy Eylar, from the office of International programs of CSU, for her invaluable advices. Additionally, I would like to thank Lincoln Mueller and Brandon Weaver from the City of Fort Collins and the New Belgium Brewing Company, respectively.

I would like to thank various friends for their support. I am especially grateful with Claudia Molina, Carolina Gutierrez, and Freddy Saavedra for being such wonderful persons.

I wish to thank my parents for their love and encouragement not only throughout my study, but my whole life. Finally, my special acknowledgment to my lovely wife and my beloved son to whom I thank for being such an inspiration in my life.

TABLE OF CONTENTS

ABSTRACT	ii
ACKNOWLEDGEMENTS	iv
Chapter 1 INTRODUCTION	1
1.1 Research motivation	1
1.2 Research objective	3
1.3 Thesis overview	3
Chapter 2 LITERATURE REVIEW	5
2.1 Anaerobic digestion	5
2.1.1 Hydrolysis and acidogenesis	5
2.1.2 Methanogenesis	6
2.1.3 Inhibition	8
2.2 Manure leachate as a source of carbon	9
2.3 High-rate reactors configuration	11
2.3.1 Upflow anaerobic sludge blanket (UASB) reactor configuration	12
2.3.2 Fixed-film reactor configuration	12
2.3.3 Hybrid reactor configuration	14
2.4 Computational fluid dynamics (CFD) applied to the design of anaerobic reactors	14
2.5 Monitoring and Operational considerations	20
2.6. Summary	21
Chapter 3 HYDRODYNAMICS CHARACTERIZATION AND OPTIMIZATION OF HIGH-RATE ANAEROBIC REACTORS BY TRACER TESTS AND COMPUTATIONAL FLUID DYNAMICS (CFD)	23
3.1 Introduction	23
3.2 Methods	24
3.2.1 Anaerobic reactors configuration	24
3.2.1 Tracer tests	27
3.2.2 Computational fluid dynamics (CFD) model	30
3.3 Results and Discussion	32

3.4 Conclusions.....	37
Chapter 4 SIMULTANEOUS INOCULATION FOR UPFLOW ANAEROBIC SLUDGE BLANKET, FIXED-FILM, AND HYBRID REACTORS	38
4.1 Introduction.....	38
4.2 Methods	39
4.2.1 Inoculation reactor configuration and start-up	39
4.2.2 Leach-bed reactor	42
4.2.3 Inoculation monitoring and operation.....	43
4.3 Results and Discussion	46
4.4 Conclusions.....	50
Chapter 5 ANAEROBIC DIGESTION PERFORMANCE OF HIGH-RATE ANAEROBIC REACTORS PROCESSING MANURE LEACHATE.....	51
5.1 Introduction	51
5.2 Methods	53
5.2.1 Reactor design and configuration.....	53
5.2.2 Performance monitoring and operation of anaerobic reactors.....	58
5.2.3 Calibration and determination of Volatile Fatty Acids (VFAs) in sludge and manure leachate by Mass Spectrometry	60
5.3 Results and Discussion.....	64
5.2 Conclusions.....	67
Chapter 6 CONCEPT DESIGN OF HIGH-RATE ANAEROBIC REACTORS TO PROCESS MANURE LEACHATE AT A PILOT SCALE	68
6.1 Introduction.....	68
6.2 Methods	69
6.2.1 Design parameters	69
6.2.2 Inlet - Outlet & Gas Collection Setup	72
6.2.3 Monitoring	73
Chapter 7 CONCLUSIONS	75
REFERENCES.....	78
Appendix A: Stock Solution for Preparation of Define Media for Monitoring Biochemical Methane Potential.....	80
Appendix B: Raw data of the inoculation reactor	81

Chapter 1 INTRODUCTION

1.1 Research motivation

Anaerobic digestion is characterized by a high degree of waste stabilization, low production of waste biological sludge, low nutrient requirements, no oxygen requirements, and the recovery of an end product such as methane, which has an important energy value (McCarty, 1964a). It has been claimed that these advantages are mostly valid for concentrated wastes, where the biochemical oxygen demand (BOD) are greater than 10,000 mg/L. Otherwise, the application of anaerobic digestion is limited and consequently unfeasible.

Suspended growth reactors are more suitable to treat high solids concentration wastewaters than high-rate anaerobic reactors when the hydrolysis of solids is the rate-limiting step (Tchobanoglous, 2003). Additionally, it is claimed that such suspended growth reactors require longer solids retention times (SRT) to handle high solids concentrations. Thus, technologies capable to allow the processing of high solids concentration waste in high-rate anaerobic reactors are needed (Sharvelle, 2012).

The selection of the most suitable reactor is strongly linked to the solids content (Sharvelle, 2012). For instance, high-rate anaerobic reactors such as the Upflow Anaerobic Sludge Blanket (UASB) and the fixed film, are required to be fed by solids content ranged from 3% to 7% and less than 3%, respectively (Sharvelle, 2012). As a result, technology such as the leachate bed reactor has been developed nowadays in order to obtain high organic leachate from high solids organic waste such as manure, which consequently could feed such high-rate anaerobic reactors (Sharvelle, 2012).

Anaerobic digestion can be summarized as the reduction of the carbon content in the organic matter to its most reduced oxidation state, which is known as methane (CH_4) (Rittmann & McCarty, 2001). Anaerobic digestion can be described by three stages; where the first stage is defined as hydrolysis, the second stage is fermentation of organic matter into organic acids and hydrogen (acidogenesis), and the third stage is conversion of organic acids and hydrogen into methane (Lawrence & McCarty, 1969).

The biodegradability of complex substrates and their further reduction to methane depends of the content of carbohydrates, lipids, and proteins (Vavilin et al., 2008). Vavilin et al states that biodegradability depends on the content of lignin (2008). It is claimed that dairy manure may be the most studied carbon source to be used in anaerobic digestion (Labatut et al., 2011). Also, the hydrolysis of cattle manure, measured by volatile fatty acids (VFAs) and soluble chemical oxygen demand (COD) has been proven to be enhanced when leach-bed reactors are used (Myint & Nirmalakhandan, 2009). Thus, a multi-stage anaerobic digestion comprised of a leachate bed reactor followed by a high-rate anaerobic reactor can improve the process as a whole (Sharvelle, 2012).

Anaerobic treatment processes include suspended growth, upflow and downflow attached growth, fluidized-bed attached growth, upflow anaerobic sludge blanket (UASB), anaerobic lagoons, and membrane separation anaerobic process (Tchobanoglous, 2003). From an economical point of view, immobilized cell reactors are more ideal to increase the ratio between the solids retention time to hydraulic retention time (SRT/HRT); (Speece, 1983). The UASB has been found to be advantageous due to the high density of its granules, high settling velocity, and high loading rate that can be handled; whereas fluidized bed reactors are characterized by high surface area and high settling velocity, and good mass transfer (Speece, 2008).

Understanding hydrodynamics in anaerobic digester reactors is key to predicting process performance. Computational fluid dynamics (CFD) has been broadly applied in the characterization, design, and optimization of bioenergy systems such as anaerobic lagoons, plug-flow digesters, complete mix digesters, anaerobic biohydrogen fermenters, anaerobic biofilm reactors, and photobioreactors (Wu, 2012). Additionally, tracer tests have traditionally been applied for the hydrodynamics characterization of reactors such as the residence time distribution, which describes the duration of water molecules that stay in the reactor (Edzwald, 2011).

1.2 Research objective

The objective of this research is compare the performance of three different reactor configurations; the Upflow Anaerobic Sludge Blanket (UASB), fixed film, and a hybrid for processing manure leachate as a carbon source. This comparison will contribute to design criteria and the most suitable technology regarding the anaerobic digestion of such carbon source. Additionally, the hydrodynamics of these reactors' configurations will be improved by the aid of computational fluid dynamics (CFD), where infinite scenarios can be evaluated upon its validation by performed tracer tests.

1.3 Thesis overview

The following chapter (Chapter 2) provides an overview of the state of the art of anaerobic digestion. Manure leachate technologies and characteristics are described. Then, the high-rate anaerobic reactors researched with the aim of determining the most suitable technology are overviewed in this chapter. Moreover, the application of CFD in anaerobic digestion will be reviewed. The third chapter (Chapter 3) covers the hydrodynamics characterization of the high-rate reactors by tracer tests as well the optimization of such reactors by the aim of CFD. The

simultaneous inoculation performed for the UASB and fixed film reactors and the anaerobic digestion of manure leachate by three high-rate anaerobic reactors are included in Chapters 4 and 5, respectively. Also, an alternate experiment is suggested in Chapter 6 to enhance the research results of Chapter 5. Last, a chapter of conclusions (Chapter 7) is dedicated to summarizing the findings and future work regarding the anaerobic digestion of manure leachate by UASB, fixed-film, and hybrid reactors.

Chapter 2 LITERATURE REVIEW

2.1 Anaerobic digestion

2.1.1 Hydrolysis and acidogenesis

Hydrolysis is described as the transformation of large complex molecules by the excretion of extracellular enzymes to be biologically available (O'Rourke, 1968). It is stated that biodegradability is dependent on the content of lignin (Vavilin et al., 2008). The content of lignocellulose in raw dairy manure was observed to be 56% (Labatut et al., 2011), which was the highest reported in this research among other substrates. Also, cattle manure has been reported hydrolyze at a rate of 0.13 day^{-1} (Vavilin et al., 2008). Hydrolysis can be modeled by the rate of VFA production during anaerobic digestion, which is depicted in Equation 2.1 for a plug flow reactor (Vavilin et al., 2008).

$$VFA = VFA_0 + \alpha VS_0 (1 - e^{-kt}) \quad \text{Equation 2.1}$$

Where:

$$VFA = VFA \text{ concentration at a given time } \left(\frac{mg}{L} \right)$$

$$VFA_0 = \text{Initial concentration of VFAs } \left(\frac{mg}{L} \right)$$

α = Conversion constant for volatile solids to hydrolysis product

VS = Initial concentration of Volatile Solids

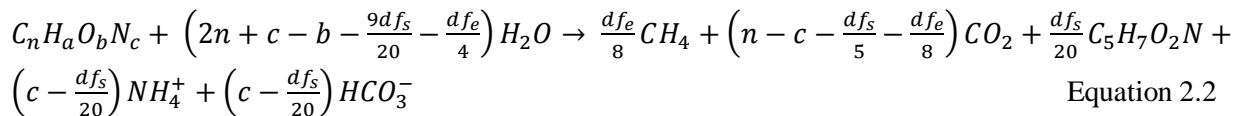
k = kinetic coefficient (day^{-1})

t = time (days)

2.1.2 Methanogenesis

Complex processes, which involve intermediate steps and a high diversity of bacteria, are carried out during anaerobic digestion as depicted in Figure 2.1 (Speece, 2008). It is stated that lignin that has not been hydrolyzed is refractory in anaerobic conditions (Tong et al., 1990), where 10% to 80% of conversion to methane was observed for various lignocellulosic materials. Biodegradability of samples can be measured by the biochemical methane potential (BMP), where samples are anaerobically added to an inoculated defined media and further incubated for about 30 days at 35°C (Owen et al., 1979). The stock solution required for the preparation of defined media is included in the Appendix A.

Alternatively, the biodegradability of samples can be measured by the specific methanogenic activity (SMA), which acetate is usually used as a substrate (James et al., 1990). However, acetate is the substrate source of about 70% of the methane produced (Valcke & Verstraete, 1983). Substrates such as dairy manure, which contains 56% of lignocellulose, depicts a slow biodegradability when plotting its cumulative biogas production during a BMP assay (Labatut et al., 2011). The amount of CH₄, HCO₃⁻, and CO₂ formed from an organic substrate can be predicted based on stoichiometry using Equation 2.2 (Rittmann & McCarty, 2001).



Where:

$$d = 4n + a - 2b - 3c$$

f_e = Fraction of electrons used for energy generation

$$f_s = f_s^0 \left[\frac{1+(1-f_d)b\theta_x}{1+b\theta_x} \right]$$

f_s = Amount of electrons used for cell synthesis

f_s⁰ = Maximum value of electrons that can be used for synthesis

f_d = Fraction of biomass that is biodegradeable

b = Endogenous-decay coefficient (day⁻¹)

θ_x = Mean cell residence time (day)

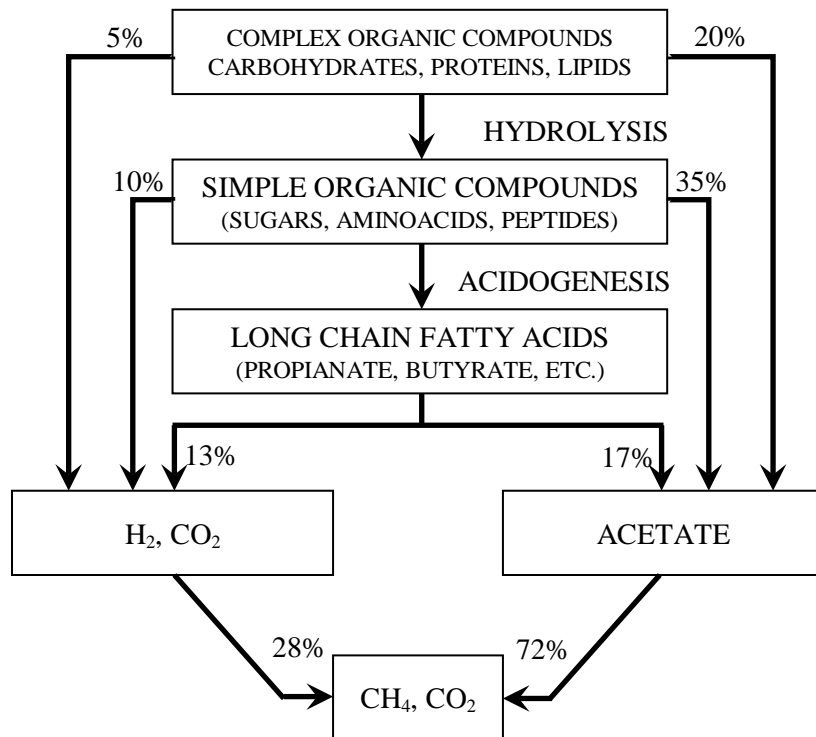
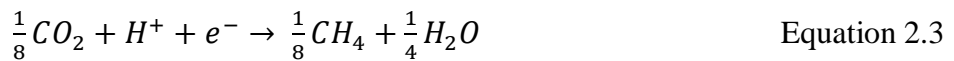


Figure 2.1 Series metabolism resulting in methanogenesis (Speece, 2008)

Under anaerobic conditions, the dominant reduction - oxidation (redox) couple can be assumed to be CO_2/CH_4 by using the half reaction shown in Equation 2.3, whereas the redox potential (pE) model is depicted in Equation 2.4 (Sawyer, 2003).



$$pE = 2.87 - pH - \frac{1}{8} \log \left(\frac{[\text{CO}_2]}{[\text{CH}_4]} \right) \quad \text{Equation 2.4}$$

Start-up and inoculation of anaerobic reactors has always been an issue in anaerobic digestion (Speece, 2012). Operators usually provide 20% of inoculum in the influent of industrial plants (Deublein, 2012). Moreover, the amount of inoculum can be determined by the ratio of mass of organic dry substance (MoTS Substract) to the mass of organic mass dry substance in the inoculum (MoTS Inoculum), which is depicted in Equation 2.5 (Deublein, 2012).

$$\frac{MoTS\ Substract}{MoTS\ Inoculum} \geq 0.5 \quad \text{Equation 2.5}$$

The relevance of soluble microbial products (SMPs) in anaerobic digestion has been pointed out due to the limitation of achieving low effluent organic levels, which mostly is constituted by SMPs in well operated anaerobic reactors (Barker & Stuckey, 2001). SMPs are outside the scope of this research.

2.1.3 Inhibition

Several organic and inorganic materials can be toxic or inhibitory during anaerobic digestion (McCarty, 1964c). As a result, the rate of substrate utilization and biomass growth are slowed by materials such as heavy metals, pesticides, antibiotics, aromatic hydrocarbons, and chlorinated solvents (Rittmann & McCarty, 2001). Anaerobic digestion is typically monitored by the rate of methanogenesis and pH; however, these parameters cannot identify the source of toxic or inhibitory issues (Speece, 2008). Also, Speece (2008) states that the concentration of VFAs can be used as a warning indicator when the process is not working correctly. Kinetics coefficients of lipids and acetic, propionic, and butyric acid for rate-limiting substrates were reported by O'Rourke (1968) (Table 2.1). It is stated that inhibition by acetic acid starts when a concentration of 1000 mg/L is presented at a pH less than 7, whereas concentrations of 50 mg/L

of isobutyric or isovaleric acid are harmful (Deublein, 2008). Also, Deublein claims that propionic acid can be toxic at concentrations of 5 mg/L; however, when the acid is undisassociated ($\text{pH}=7$), it can be toxic at a concentration of 700 mg/L (2008). Additionally, inhibition by other compounds has broadly been reported. For instance, a concentration of ammonia nitrogen ranging from 1500 to 3000 mg/L causes inhibition when pH ranged from 7.4 to 7.6, while concentrations above 3000 mg/L are considered toxic (McCarty, 1964c). As a matter of fact, ammonia has been an issue in feedstock due to the presence of proteins (Speece, 2008). Regarding inhibition by sodium (Na^+), Speece states that this cation has been observed to be a problem at 2000 mg/L; however, the methane conversion is gradually inhibited at concentrations of 10,000 mg/L (2008).

Table 2.1. Comparison of kinetic coefficients for rate-limiting substrates (O'Rourke, 1968)

Temp (°C)	Acetic		Propionic		Butyric		Lipids	
	K^* (day $^{-1}$)	K_s^{**} mg/L as COD	K (day $^{-1}$)	K_s mg/L as COD	K (day $^{-1}$)	K_s mg/L as COD	K (day $^{-1}$)	K_s mg/L as COD
35	6.1	164	9.6	71	15.6	16	6.67	2000
25	4.7	930	9.8	1140	-	-	4.65	3720
20	3.6	2130	-	3860	-	-	3.85	4620

*Maximum substrate utilization rate

**Concentration giving one-half the maximum rate

2.2 Manure leachate as a source of carbon

The chemical composition, in volatile solids mass basis, of raw dairy manure has been reported to be 3.5% VFAs, 5.7% of protein, 16.1% of lipids, 9.6% of hemicelluloses, 32.6% of cellulose, 13.8% of lignin, and a percentage of sugars, starch, and pectin of 16.5% (Labatut et al., 2011). Additionally, Labatut states that the ratio of biochemical oxygen demand (BOD) to the COD (BOD/COD) is 0.47 in manure separated liquid, whereas this ratio is observed to be 0.36 in raw

dairy manure. Moreover, hydrolysis of cattle manure, measured by VFAs and soluble COD has been proven to be enhanced by 15% and 8%, respectively, when leach-bed reactors are used (Myint & Nirmalakhandan, 2009).

A multi-stage anaerobic digester (MSAD) has been proposed to obtain high organic leachate from high solids organic waste (Sharvelle, 2012). In such technology, waste with more than 40% solids content is disposed in a leachate bed reactor, where the digested liquid from an anaerobic reactor is recycled to the substrate, thus high organic leachate with low solids contents is obtained by percolation. As a result, leachate with low solids content can be supplied to high-rate anaerobic reactors. Sharvelle states that this technology is not only suitable to deal with high solids content organic waste, greater than 40%, but also to separate the hydrolysis and methanogenesis stages (Figure 2.2) (2012).

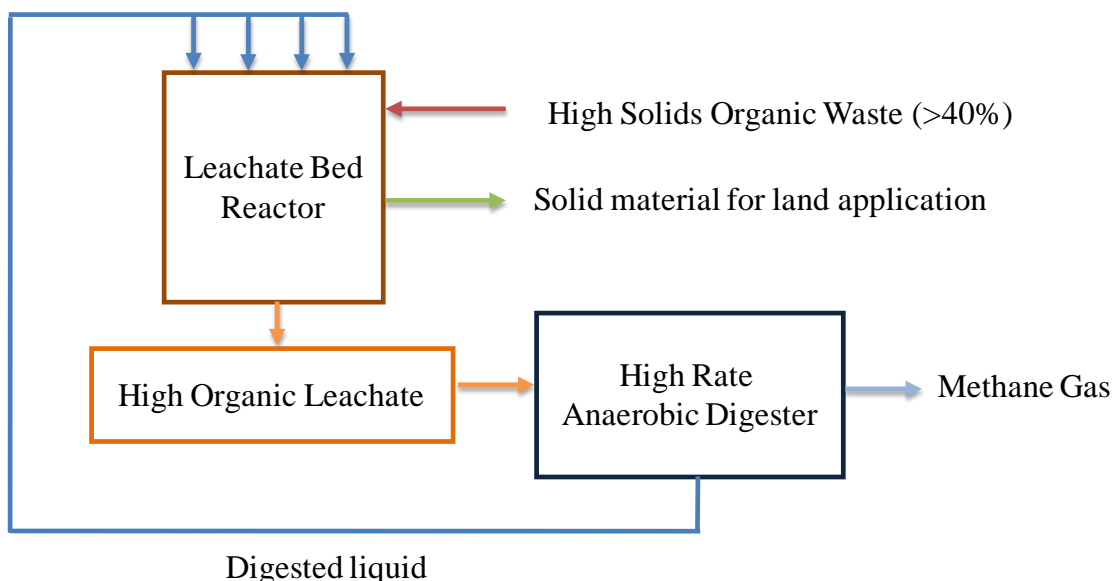


Figure 2.2 Overview of the multi-stage anaerobic digestion (MSAD) process (Sharvelle, 2012)

2.3 High-rate reactors configuration

Conventional AD technology is limited in that the hydraulic retention time (HRT) is the same as solids retention time (SRT) because biomass exits the reactor with effluent material. Because methanogens are very slow growers, high reactor volumes are required to ensure adequate SRT. High rate AD reactors address this issue by retaining biomass within them. Speece (2008) states that the favorable conditions to high concentration anaerobic biomass immobilization are fixed surfaces or media that promotes the growing of biomass (2008). Additionally, maintaining high settling rate granules and non-turbulent flows, at the inlets and the upper sections of reactors, contribute to the development of high density biomass (Speece, 2008). The high-rate anaerobic reactors evaluated in this research are explained in the next sections, while the design parameters such as hydraulic retention time (HRT), hydraulic loading rate (HLR), and organic loading rate (OLR) are summarized in Table 2.2.

Table 2.1. Design parameters of high-rate anaerobic reactors (Tchobanoglous, 2003)

High-rate anaerobic reactor	HRT (Hours)	HLR (m ³ /m ² -hr)	OLR (kg/m ³ -d)
Upflow anaerobic sludge blanket (UASB)	6	0.7 – 1.5	15 - 30
Upflow packed bed reactors (PBR)	0.9 - 3*	2	1 - 6
Fluidized-bed reactor (FBR)	12**	20 – 24	10** - 20
Hybrid	50	**	6

* Reported values for different industrial wastewaters

**Reported value for glucose

***HLR is not available in the current literature.

2.3.1 Upflow anaerobic sludge blanket (UASB) reactor configuration

The first upflow anaerobic sludge blanket (UASB) reactor was developed by Lettinga in the Netherlands in 1979, which could handle high loading rates up to $30 \text{ kg/m}^3\text{-d}$ (Speece, 1983). Speece claims that the UASB was later modified by McCarty in what he called the baffled reactor (1983). The original UASB process is depicted in Figure 2.3 (Tchobanoglous, 2003).

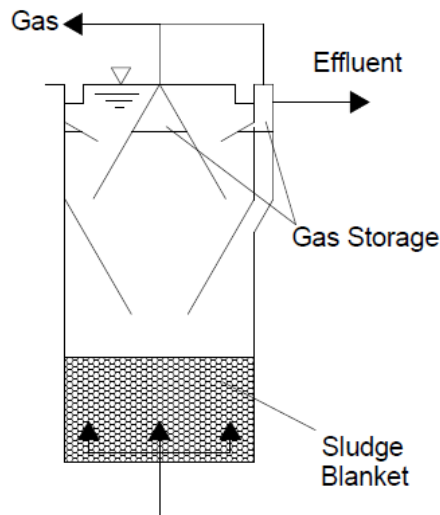


Figure 2.3 Scheme of the UASB process

Adapted from Tchobanoglous, 2003

At 35°C , an organic volumetric loading rate ranged from 15 to $24 \text{ kg/m}^3\text{-d}$ and a daily average hydraulic retention time (HRT) of 6 hours is recommended (Lettinga, 1991). Also, hydraulic loading rates (HLR) or upflow velocities ranged from 0.7 to 1.5 m/h are typically used (Tchobanoglous, 2003). Last but not least, it is suggested that large granules of initial inoculum are applied to start-up the UASB reactor (Speece, 2008).

2.3.2 Fixed-film reactor configuration

In one of the first studies of upflow packed bed reactors (PBR) in the United States, the packing material was found to have high surface area, and the Reynolds number was kept low to

contribute to reduce turbulence in the system and allow settling of unattached microorganisms (Speece, 1983). Also, Speece claims that unattached microorganisms on the packing material as biofilm, are kept in the interstices of the media (1983). This reactor can operate at organic loading rates ranged from 1 to 6 kg/m³-d (Tchobanoglous, 2003). Tchobanoglous states that the upflow attached growth anaerobic expanded bed reactor (EBR) is known for having 20% of bed expansion by keeping an upflow HLR of 2 m/h, whereas the attached growth anaerobic fluidized-bed reactor (FBR) requires upflow HLR from 20 to 24 m/h to reach 100% of bed expansion (2003). This reactor can operate at organic loading rates ranged from 10 to 20 kg/m³-d (Tchobanoglous, 2003). Additionally, it is stated that the upflow packed reactors have presented the fastest inoculation among other configurations (Speece, 2008). These three configurations for fixed-film reactors are shown in the Figure 2.4 (Tchobanoglous, 2003).

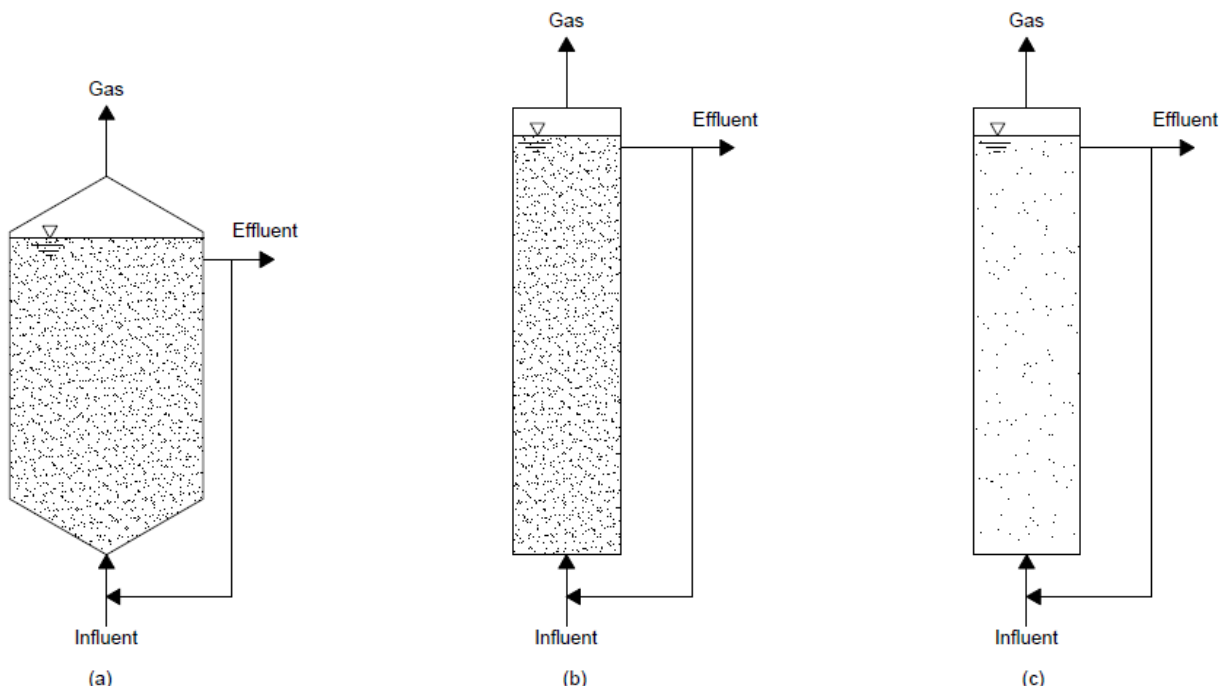


**Figure 2.4 (a) Anaerobic upflow packed-bed reactor (b) anaerobic expanded-bed reactor
(c) anaerobic fluidized-bed reactor**

Adapted from Tchobanoglous, 2003

2.3.3 Hybrid reactor configuration

Additionally, the upflow packed-bed anaerobic reactors can be design as a hybrid configuration, where the upper depth of the column is filled by 50 to 70% of packing material (Tchobanoglous, 2003). Moreover, this configuration can enhance the retention of biomass when the bottom is design unpacked as an UASB, and the top is packed with material (Speece, 2008). Limited research is available in regards with design parameters of hybrid reactors. Speece reported the design parameters of a 3400 m³ hybrid reactor with a 1/3 unpacked bottom and a 2/3 packed upper side with corrugated plastic media, which surface area is 125 m²/m³. This reactor is fed with aspartame wastewater of 18,000 mg/l COD and its biomass concentration at the bottom is 50,000 to 100,000 mg/l of volatile suspended solids (VSS). Also, the designed HRT is 50 hours, whereas the organic loading rate (OLR) is 6 kg/m³-d, removing 80% of the COD.

2.4 Computational fluid dynamics (CFD) applied to the design of anaerobic reactors

CFD is often applied to better understand the hydraulics of reactors. The UASB reactor has been already modeled by an Eulerian approach in CFD, whereas the approach followed during simulations of the FBR by CFD is not fully documented (Wang et al., 2010). Additionally, the HRT was computed from a CFD model in a complete stirred tank reactor (CSTR) (Meroney & Colorado, 2009). Moreover, the residence time distribution (RTD) of a tubular stirred reactor was computed in the CFD model known as Fluent-ANSYS and validated by tracer tests (Cao et al., 2009).

The Reynolds number is defined as the ratio of the inertial forces to the viscous forces of a fluid. The inertial forces include density, average velocity and the length of the reactor, while the viscous force is essentially the viscosity, as shown in equation 2.6 (Çengel & Cimbala, 2010). Physically, when larger Reynolds numbers (Re) are developed, the inertial forces are larger than

the viscous force so the highly disordered layers formation is not stopped by the viscosity of the fluid (Çengel & Cimbala, 2010). On the other hand, Çengel & Cimbala state that when a relatively small Reynolds number is observed, a stronger shear force is developed by the viscous force; thus, smooth layers are more likely to be formed (2010).

$$Re = \frac{V_{avg}D}{\nu} = \frac{\rho V_{avg}D}{\mu} \quad \text{Equation 2.6}$$

Where:

V_{avg} = Average velocity, m/s

D = Length of the reactor, m

ρ = Density, kg/m³

ν = Kinematic viscosity, m²/s

μ = Dynamic viscosity, kg/m s

Based on the Reynolds number, the flow is classified as laminar when its value is less than or equal to 2300, while the flow becomes turbulent when this value turns out to be equal to or greater than 4000. Thus, any value between the laminar and turbulent flow is classified as a flow in transition (Çengel & Cimbala, 2010).

The finite volume method, where control volumes are cell centered, is used by CFD models of ANSYS to solve the transport equation for mass, momentum, energy, and species (ANSYS, 2011a). The transport equation presents different transport process such as the rate of change with respect to time, convection, diffusion, and sources, which are depicted in the Equations 2.7 and 2.8 (Versteeg, 2007).

$$\text{Rate of Increase of } \phi \text{ of fluid element} + \text{Net rate of flow of } \phi \text{ out of fluid element} = \text{Rate of increase of } \phi \text{ due to diffusion} + \text{Rate of increase of } \phi \text{ due to sources} \quad \text{Equation 2.7}$$

$$\int_{CV} \frac{\partial(\rho\phi)}{\partial t} dV + \int_{CV} \operatorname{div}(\rho\phi u) dV = \int_{CV} \operatorname{div}(\Gamma \operatorname{grad} \phi) dV + \int_{CV} S_\phi dV \quad \text{Equation 2.8}$$

Where:

ϕ = scalar or tracer of known concentration

ρ = Density

u = Velocity vector

Γ = Diffusion coefficient

S_ϕ = Source term

CV = Control volume

Therefore, the partial differential equations are discretized to obtain linear algebraic equations, which can be made by ANSYS Meshing (ANSYS, 2011a). Additionally, quality criteria of the mesh developed in ANSYS for FLUENT includes the skewness and the orthogonal quality (ANSYS, 2011c). The skewness is computed by two methods, which are depicted in equations 2.9 and 2.10, respectively, whereas the orthogonal quality (OQ) for a cell is the minimum value obtained by the equation 2.11 (ANSYS, 2011c). Also, ANSYS states that it is typical to keep a minimum orthogonal quality of 0.1 or a maximum skewness of 0.95 (2011).

$$\text{Skewness} = \frac{\text{optimal cell size} - \text{cell size}}{\text{optimal cell size}} \quad \text{Equation 2.9}$$

$$Skewness = \max \left[\frac{\theta_{max} - \theta_e}{180 - \theta_e}, \frac{\theta_e - \theta_{min}}{\theta_e} \right] \quad \text{Equation 2.10}$$

$$\frac{A_i \cdot f_i}{\left| \vec{A}_i \right| \left| \vec{f}_i \right|} \frac{A_i \cdot C_i}{\left| \vec{A}_i \right| \left| \vec{C}_i \right|} \quad \text{Equation 2.11}$$

Where,

θ_e = The equiangular face/cell, which is 60° for tetrahedrons triangles, and 90° for quadrilaterals and hexahedrons

θ_{max} = The maximal internal angle of the cell

θ_{min} = The minimal internal angle of the cell

A_i = Face normal vector

f_i = Vector from the centroid of the cell to the centroid of the face

C_i = Vector from the centroid of the cell to the centroid of adjacent cell

Moreover, the transport of a random scalar in a single phase flow, which can be named ϕ_k , can be modeled by Fluent by solving Equation 2.12, where Γ_k and S_ϕ are the diffusion coefficient and source term, respectively (ANSYS, 2011b).

$$\frac{\partial \rho \phi_k}{\partial t} + \frac{\partial}{\partial x_i} \left[\rho u_i \phi_k - \Gamma_k \frac{\partial \phi_k}{\partial x_i} \right] = S_\phi \quad k = 1, \dots, N \quad \text{Equation 2.12}$$

Moreover, CFD models, in which this research addresses the hydrodynamics characteristics of reactors, must be validated by experimentation (Venayagamoorthy, 2012), called in this case tracer tests. The hydrodynamic characteristics of reactors can be described by tracer tests through two different methods; a pulse input tracer test where a known mass is injected at one instant, or a step input tracer test where a steady concentration is added continuously (Edzwald, 2011) . A tubular reactor with dispersion can be simulated such that the Peclet number, which is depicted

in the Equation 2.13, tends to the infinite, whereas the dispersion coefficient tends to zero (Perry, 2008).

$$Pe = \frac{uL}{D} \quad \text{Equation 2.13}$$

Where:

Pe = Peclet number

u = Linear velocity, m/s

L = Reactor length, m

D = Dispersion coefficient, m^2/s

Thus, an ideal plug flow reactor would present an exit age distribution and a cumulative age distribution as depicted in Figure 2.4. The exit age distribution, which is computed by equation 2.14, describes how the residence time of molecules of water are distributed in the reactor, while the cumulative age distribution, computed by Equation 2.15, depicts the total fraction of water that stays in the reactor at a given cumulative time (Edzwald, 2011). Last but not least, Edzwald states that from the Exit and Cumulative age distribution plots that are obtained from the tracer tests, the average hydraulic detention time can be computed by Equation 2.16.

$$E(t) = \frac{Q}{M} C_p(t) \quad \text{Equation 2.14}$$

$$F(t) = \int_0^t E(t) dt \quad \text{Equation 2.15}$$

$$\bar{t} = \frac{\sum_{all\ i} t_{i,ave} E_{i,ave} \Delta t_{i,int}}{\sum_{all\ i} E_{i,ave} \Delta t_{i,int}} \quad \text{Equation 2.16}$$

Where:

Q = Flow rate

M = Mass

$C_p(t)$ = Concentration of the tracer in the effluent

$E(t)$ = Exit age distribution

$F(t)$ = Cumulative age distribution

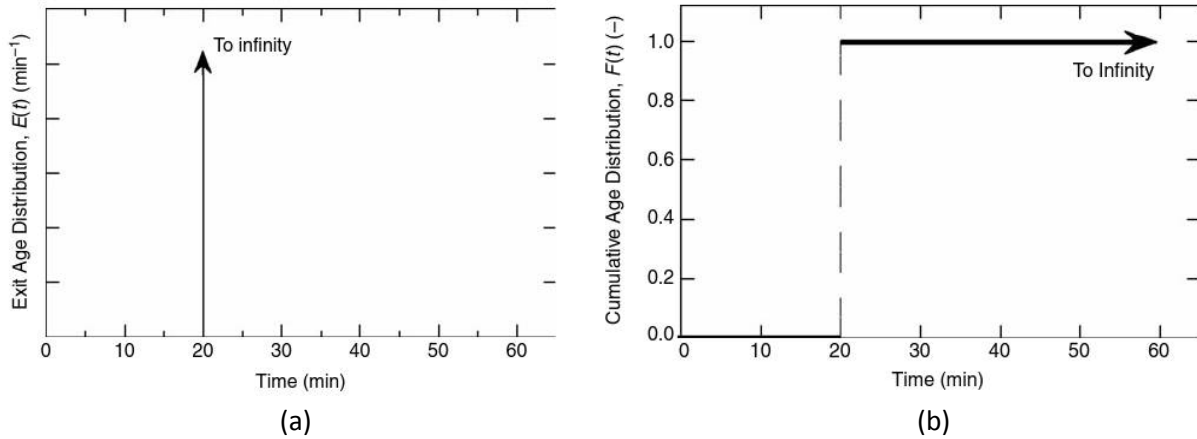


Figure 2.4 (a) Exit age distribution for an ideal plug flow reactor (b) cumulative age distribution for an ideal plug flow reactor (Edzwald, 2011)

Additionally, Tchobanoglous states that the theoretical residence time is computed by Equation 2.17, while the Morrill dispersion index (MDI) is computed by Equation 2.18 (2003). Moreover, it is claimed that MDI of an ideal plug flow reactor is 1.0; however, an MDI of 2.0 or less is believed to be an effective plug flow reactor by the Environmental Protection Agency (EPA) (Tchobanoglous, 2003).

$$\tau = \frac{V}{Q} \quad \text{Equation 2.17}$$

$$MDI = \frac{t_{90}}{t_{10}}$$
Equation 2.18

Where:

τ = theoretical residence time

V = Volume

Q = Flow rate

t_{90} = Time at which 90% of the tracer had passed through the reactor

t_{10} = Time at which 10% of the tracer had passed through the reactor

2.5 Monitoring and Operational considerations

It is claimed that the solids retention time, also known as cell residence time, is the most important parameter regarding the efficiency and operation of the anaerobic digestion, which is shown in Equation 2.19 (McCarty, 1964a).

$$SRT = \frac{M_t}{M_e}$$
Equation 2.19

Where:

SRT = Solids retention time

M_t = Total weight of suspended solids in treatment system

M_e = Total weight of suspended solids leaving the system per day, including both the deliberately wasted and that passing out with the plant effluent

It is stated that the simplest indicators of unbalanced treatment are the increasing of volatile acids concentrations and percentage of CO_2 , and the decreasing of pH, total gas production, and waste stabilization (McCarty, 1964b). Ideal conditions, depicted in the Table 2.3, are recommended for the hydrolysis / acidogenesis and Methanogenesis stages, respectively (Deublein, 2008).

Table 2.3. Ideal conditions for anaerobic digestion (Deublein, 2008)

Parameter	Hydrolysis / acidogenesis	Methane formation
Temperature	25 – 35 °C	Mesophilic: 32 – 42 °C Thermophilic: 50 – 58 °C
pH	5.2 – 6.3	6.7 – 7.5
C:N ratio	10 – 45	20 – 30
DM content	< 40% DM	< 30% DM
Redox potential	+400 to -300mV	< -250
Required C:N:P:S ratio	500:15:5:3	600: 15:5:3
Trace elements	No especial requirements	Essential: Ni, Co, Mo, Se

Additionally, the steps suggested for troubleshooting during anaerobic digestion are summarized by maintaining pH near neutrality, determining cause of unbalance, correcting cause of unbalance, and providing pH control until treatment returns to normal (McCarty, 1964b). Also, since clogging has been an issue in high rate anaerobic reactors, it is known that an anaerobic filter located in Texas was successfully maintained by the addition of nitrogen gas, which creates turbulence in the system and release of biomass that could accumulated in excess (Speece, 2008). Last but not least, the BMP assay can be applied as a process performance test in the effluent of reactors to evaluate the capability of further anaerobic digestion in the system (Speece, 2012).

2.6. Summary

In this chapter, literature regarding anaerobic digestion was reviewed. Selected topics of environmental biotechnology and computational fluid dynamics were the focus because these elements are transcendental in the success of anaerobic digestion reactors. A multi-stage anaerobic digestion (MSAD) process is under development by Dr. Sharvelle's research group to divide the process in three stages; hydrolysis and acidogenesis, and acetogenesis and methanogenesis. This division both enables anaerobic digestion of high solids organic wastes while also producing organic leachate which can meet the solids content required by high-rate anaerobic reactors. High-rate anaerobic reactors have been stated to be more advantageous in

terms of biomass retention; however, actual literature with regards to anaerobic digestion of manure leachate by such reactors is not available. Thus, the required OLR and HRT for the UASB, PBR, FBR, and hybrid are unknown. Also, the influence of HLR on the hydrodynamics of high-rate anaerobic reactors have not been extensively researched. Nowadays, hydrodynamics of reactors can be computed by CFD models, which not only provides better understanding of the hydraulics of reactors, but also enhances design by emulating the tracer tests. Inoculation and start-up of anaerobic digesters need to have special care to guarantee the success of the process over long durations. This process has not been completely researched yet for commonly digested substrates by anaerobic reactors, thus it has not been previously investigated for manure leachate anaerobic digestion. The success of anaerobic digestion of manure leachate by high-rate anaerobic digestion will be proven by applying the available literature in regards with hydrodynamics of reactors, inoculation of high-rate anaerobic reactors, and the design judgments for such reactors.

Chapter 3 HYDRODYNAMICS CHARACTERIZATION AND OPTIMIZATION OF HIGH-RATE ANAEROBIC REACTORS BY TRACER TESTS AND COMPUTATIONAL FLUID DYNAMICS (CFD)

3.1 Introduction

Computational fluid dynamics (CFD) has been broadly applied in the characterization, design, and optimization of bioenergy systems such as anaerobic lagoons, plug-flow digesters, complete mix digesters, anaerobic biohydrogen fermenters, anaerobic biofilm reactors, and photobioreactors (Wu, 2012). The upflow anaerobic sludge blanket (UASB) reactor has been already modeled by an Eulerian approach in CFD, whereas the approach followed during simulations of the fluidized bed reactor (FBR) by CFD is not fully documented (Wang et al., 2010). Also, Wang reported an error within 10% when modeling velocities and hydraulic retention times (HRT) of reactors (2010). HRT was computed from a CFD model in a complete stirred tank reactor (CSTR) (Meroney & Colorado, 2009). In addition, the residence time distribution (RTD) of a tubular stirred reactor was computed in the CFD model known as FLUENT-ANSYS and validated by tracer tests (Cao et al., 2009). The literature review done in this research show that hydrodynamics of reactors has already been simulated by CFD; however, the influence of hydraulic loading rates (HLR) in the hydrodynamics of high-rate anaerobic reactors has not been evaluated by CFD and validated by tracer tests.

Hydraulic loading rates (HLR) or upflow velocities recommended for UASB reactors range from 0.7 to 1.5 m/h (Tchobanoglous, 2003). Also, Tchobanoglous states that the upflow attached growth anaerobic expanded bed reactor (EBR) is known for having 20% of bed expansion by keeping and upflow HLR of 2 m/h, whereas the attached growth anaerobic fluidized-bed reactor (FBR) requires upflow HLR up to 20 m/h to reach 100% of bed expansion (2003). Moreover, it

was reported that an anaerobic fixed-film reactor was predominated by dispersion and dead zones at low flow rates, whereas a plug flow behavior, small dispersion, and reduction of dead zones were found at higher flow rates. (Méndez-Romero et al., 2011).

Tchobanoglou (2003) claims that the Morril Dispersion Index (MDI) of an ideal plug flow reactor is 1.0; however, an MDI of 2.0 or less is believed to be an effective plug flow reactor by the Environmental Protection Agency (EPA). Therefore, the objective of this research is not only to characterize the hydrodynamics of three high rate anaerobic reactors intended to treat manure leachate, but also to indentify the best HLR, in a given range, capable to reduce dead zones and approach an ideal plug flow reactor. The three reactors to be modeled are the UASB, the upflow packed-bed reactor (PBR), and a hybrid alternative, where the bottom of the hybrid alternative's design is unpacked as an UASB, and the top is packed with plastic material. At first, the hydrodynamics characterization was performed by tracer tests. Afterwards a CFD model was developed, which was validated by the tracer tests. Thus, the best hydrodynamics conditions of the high-rate reactors were identified by through use of CFD.

3.2 Methods

3.2.1 Anaerobic reactors configuration

Three high-rate reactors were evaluated in this research; the UASB, fixed-film, and a hybrid alternative. The reactors were made with acrylic tubes of 2.19 meters in length, a diameter of 19.2 centimeters, and a cross section area of 290 cm² (Figure 3.1 (a)). Inside-of-pipe grippers made with glass-reinforced ABS plastic and a diameter of about 19 centimeters were used to adapt an influent and effluent to the columns (Figure 3.1 (b)). The grippers (Figure 3.1(c)) are equipped by large zinc wing nut, natural rubber o-ring, and galvanized carriage bolt to prevent corrosion. The gripper mass is 1.37 kg and is capable to handle up to 12 meters of back pressure.

Five, 3.2 mm diameter holes were drilled in the influent gripper, while ten 6.4 mm holes were drilled in the effluent. The inlet and outlet were provided by hose bars and vinyl tubing. Also, a HDPE funnel was used to emulate the gas collection system, which was not operating during the tracer tests by closing a valve because the liquid phase is the one to be modeled in this research. The fixed-film and hybrid reactors configurations were also provided by plastic media. 1.83 meters of depth was filled by plastic media in the fixed film reactor, whereas the upper section of the hybrid reactor was filled by 0.64 meters of plastic media. The media was provided by Entex Technologies Inc (Table 3.1). The plastic media is depicted in the Figure 3.2.

Table 3.1. Technical specifications of plastic media

Surface area	16.6 m ² /m ³
Cylinder diameter	17.78 mm
Cylinder length	13.97 mm
Weight	136.15 kg/m ³
Specific gravity	0.92 – 0.96
Void space	0.85

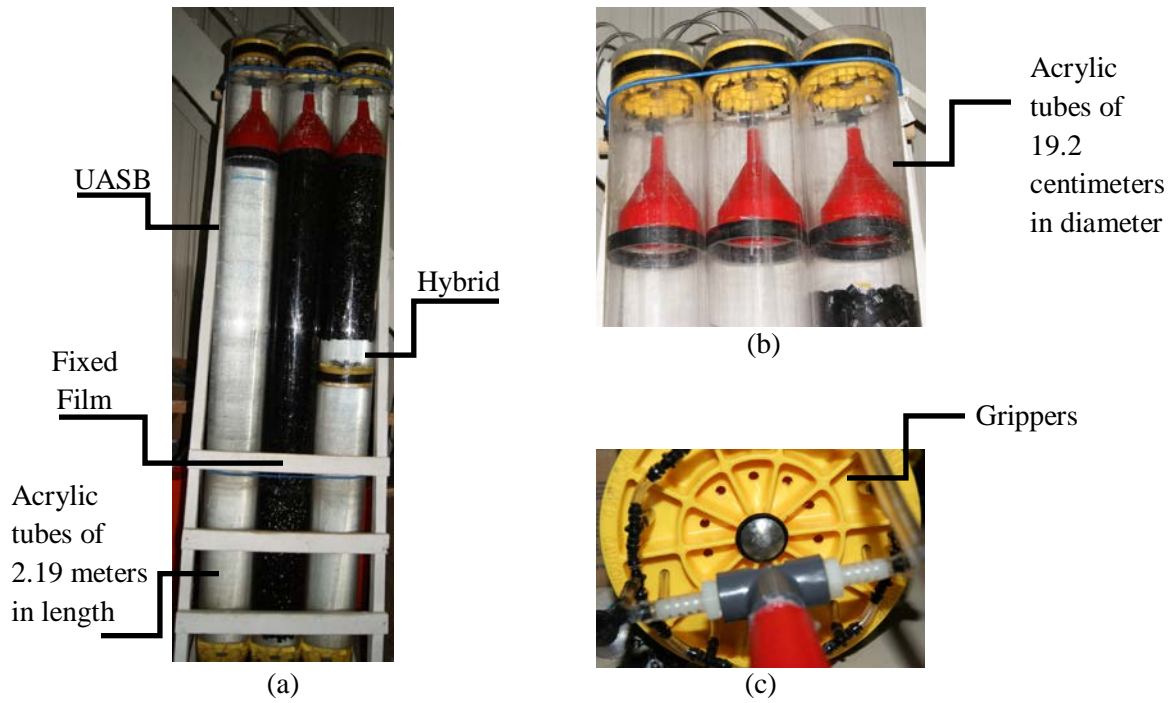


Figure 3.1 (a) Anaerobic reactors (b) Gas collection system (c) Effluent



Figure 3.2 Plastic media used in the fixed-film and hybrid reactors

3.2.1 Tracer tests

Two tracer tests were carried out for each reactor. Tap water was selected as the fluid, while sodium chloride (NaCl) was chosen as the tracer due to its conservativeness and low cost of its measurement. The electrical conductivity (EC) of the tap water used for the tracer test of the UASB reactor during the first and second test were 115 and 143 μS , respectively. The EC of the tap water used for the two tracer tests performed for the fixed-film were 143 and 121 μS . Finally, the EC found during the two tracer tests for the hybrid reactor were 137 and 123 μS . These EC values were used as a baseline when computing the effluent concentration profile, exit age distribution, and cumulative age distribution. Since inhibition in anaerobic digestion may start at a concentration of Na^+ of 2000 mg/L (Speece, 2008), the pulse input tracer test method was selected, where a known mass is injected at one instant (Edzwald, 2011).

The first tracer test of the UASB reactor was done at a hydraulic loading rate (HLR) of 0.829 $\text{m}^3/\text{m}^2\text{-h}$, which is within the recommended interval ranged from 0.7 to 1.5 $\text{m}^3/\text{m}^2\text{-h}$, while the second test was subjected to a HLR of 0.306 $\text{m}^3/\text{m}^2\text{-h}$. The EC in the effluent were measured at intervals of 0.5 hour. On the other hand, the fixed-film reactor were tested initially at an HLR of 0.306 $\text{m}^3/\text{m}^2\text{-h}$, which is below 2 $\text{m}^3/\text{m}^2\text{-h}$ as recommended for packed-bed reactor (PBR) but achievable with the available pump described later in this method, and then at a HLR of 10.6 $\text{m}^3/\text{m}^2\text{-h}$ emulating a fluidized-bed reactor (FBR), where the EC were measured at intervals of 30 minutes and 2 to 4 minutes, respectively. Finally, the tracer tests for the hybrid reactor were done at HLR of 0.340 $\text{m}^3/\text{m}^2\text{-h}$ and 12.450 $\text{m}^3/\text{m}^2\text{-h}$ at the same intervals performed for the fixed-film reactor. The second tracer tests carried on the fixed-film and hybrid reactors stayed below the recommended values for FBR, which is 20 $\text{m}^3/\text{m}^2\text{-h}$. These HLR were chosen due to the recommended values in the literature review and what was achievable by available pumps.

The pump used for the tracer tests of the UASB reactor and the lowest HLR of the fixed film and hybrid reactors was a motor driven diaphragm dosing pump MEMDOS E/DX of JESCO, whereas the tracer tests for the highest HLR of the fixed-film and hybrid reactor were equipped with the peristaltic pump Master Flex I/P Model 77600-62 and a high capacity pump controller model 7591-60. The peristaltic pump was used to achieve the higher HLRs since it had more capacity than the diaphragm pump. The EC was measured in the effluent of the reactors by using the HI 8733 Conductivity Meter. Additionally, calibration curves for low and high HLR, respectively, were created (Figure 3.3). Two different calibration curves were necessary since high HLR requires higher concentrations of the tracer due to the low hydraulic retention time (HRT).

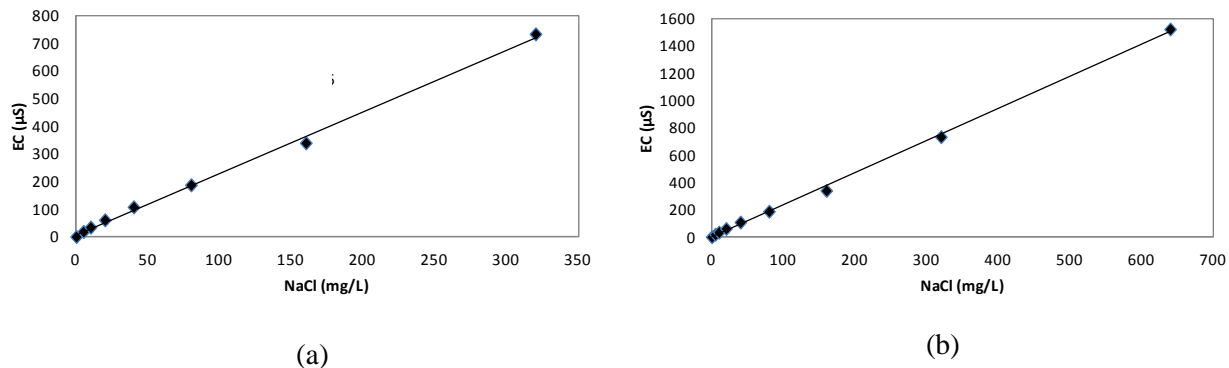


Figure 3.3 Calibration curves for EC (a) Low HLR ($R^2=0.9976$) (b) High HLR ($R^2=0.9987$).

The EC measured in the effluent of the reactors were measured until steady state was reached. Steady state was defined to be achieved when at least three measurements in a row varied by less than 10%; however, most of the tracer tests showed a difference of about 5% during the defined steady state conditions. Consequently, the effluent concentration profile was computed from the

raw data and the calibration curves. Then, the exit age distribution was computed by equation 3.1, while the cumulative age distribution was computed by Equation 3.2. (Edzwald, 2011). From the Exit and Cumulative age distribution plots that were obtained from the tracer tests, the average hydraulic detention time can be computed by Equation 3.3 (Edzwald, 2011).

$$E(t) = \frac{Q}{M} C_p(t) \quad \text{Equation 3.1}$$

$$F(t) = \int_0^t E(t) dt \quad \text{Equation 3.2}$$

$$\bar{t} = \frac{\sum_{all\ i} t_{i,ave} E_{i,ave} \Delta t_{i,int}}{\sum_{all\ i} E_{i,ave} \Delta t_{i,int}} \quad \text{Equation 3.3}$$

Where:

Q = Flow rate

M = Mass

$C_p(t)$ = Concentration of the tracer in the effluent

$E(t)$ = Exit age distribution

$F(t)$ = Cumulative age distribution

Last but not least, the theoretical residence time was computed by Equation 3.4, while the Morrill dispersion index (MDI) was computed by Equation 3.5 (Tchobanoglou, 2003).

$$\tau = \frac{V}{Q} \quad \text{Equation 3.4}$$

$$MDI = \frac{t_{90}}{t_{10}} \quad \text{Equation 3.5}$$

Where:

τ = theoretical residence time

V = Volume

Q = Flow rate

t_{90} = Time at which 90% of the tracer had passed through the reactor

t_{10} = Time at which 10% of the tracer had passed through the reactor

3.2.2 Computational fluid dynamics (CFD) model

The strategy for CFD simulations includes pre-processing, solver settings, and post-processing (Wu, 2012). Wu (2012) states that pre-processing encompasses the geometry design and meshing, whereas solver settings deals with the physical model, properties, initial and boundary conditions. Post-processing involves interpretation of the results generated by the CFD model. The geometry design for this research was done in AutoCAD 2012. A three-dimensional (3D) model was designed in AutoCAD for the UASB reactor and also built for this research (Figure 3.4), where the relevant components of its geometry regarding the residence time distribution (RTD) and hydraulic retention time (HRT) of the liquid phase is included.

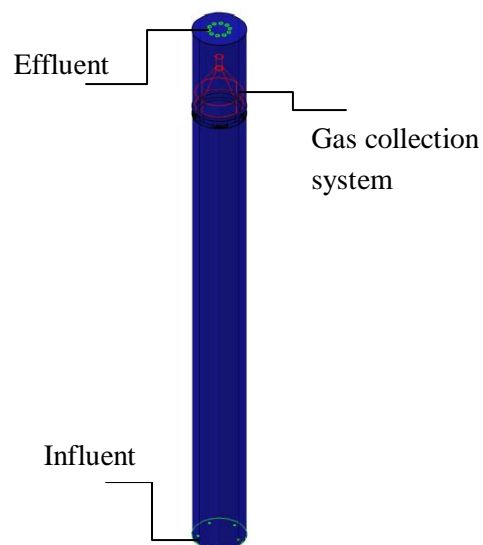


Figure 3.4 3D design of the UASB reactor

Designed in AutoCAD 2012

The partial differential equations of transport, shown in equations 3.6 and 3.7 (Versteeg, 2007), are discretized to obtain linear algebraic equations (ANSYS, 2011a). The discretization was developed by ANSYS Meshing, where a minimum orthogonal quality of 0.1 and a maximum skewness of 0.95 were applied (ANSYS, 2011c).

$$\begin{array}{l} \text{Rate of} \\ \text{Increase} \\ \text{of } \phi \text{ of fluid} \end{array} + \begin{array}{l} \text{Net rate of flow} \\ \text{of } \phi \text{ out of fluid} \\ \text{element} \end{array} = \begin{array}{l} \text{Rate of increase} \\ \text{of } \phi \text{ due to} \\ \text{diffusion} \end{array} + \begin{array}{l} \text{Rate of increase} \\ \text{of } \phi \text{ due to} \\ \text{sources} \end{array} \quad \text{Equation 3.6}$$

$$\int_{CV} \frac{\partial(\rho\phi)}{\partial t} dV + \int_{CV} \operatorname{div}(\rho\phi u) dV = \int_{CV} \operatorname{div}(\Gamma \operatorname{grad} \phi) dV + \int_{CV} S_\phi dV \quad \text{Equation 3.7}$$

The geometry was discretized by the CutCell method, which generated 91,407 nodes and 83,755 elements. Moreover, the obtained orthogonality quality was 0.154, whereas the skewness was 0.958. The meshing obtained is depicted in the Figure 3.5.

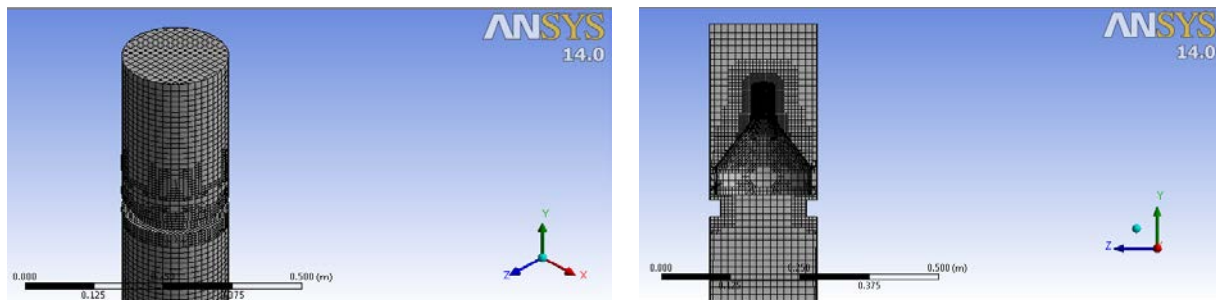


Figure 3.5 Meshing of the UASB reactor

Solver settings were developed in the CFD code Fluent, where the transport of a scalar or tracer is modeled by solving Equation 3.8 (ANSYS, 2011b). Since the Reynolds numbers for the

minimal and maximal HLR to be modeled in the UASB are 9,648 and 48,893, respectively, the standard k- ϵ turbulence model with standard wall functions was used for the calculations, which has been reported to be effective in similar research (Meroney & Colorado, 2009). Also, the SIMPLE method was chosen and the second order upwind discretization method was selected to solve the discretized terms. The solutions were considered to converge when scaled residuals reached values below 10^{-3} .

$$\frac{\partial \rho \phi_k}{\partial t} + \frac{\partial}{\partial x_i} \left[\rho u_i \phi_k - \Gamma_k \frac{\partial \phi_k}{\partial x_i} \right] = S_\phi \quad k = 1, \dots, N \quad \text{Equation 3.8}$$

The residence time distribution obtained from the CFD model was validated by comparing results to the Morril Dispersion Index (MDI) and the average hydraulic detention time computed by tracer tests. Last but not least, the CFD model was applied to investigate the best hydrodynamics conditions at various HLRs.

3.3 Results and Discussion

The MDI was determined for each reactor under each HLR tested to determine whether plug flow conditions were observed. The MDI of an ideal plug flow reactor is 1.0; however, an MDI of 2.0 or less is believed to be an effective plug flow reactor (Tchobanoglous, 2003). The exit age distribution and cumulative age distribution were computed for the three high-rate reactors. The UASB reactor was characterized by plug flow conditions when a low HLR, such as $0.296 \text{ m}^3/\text{m}^2\text{-h}$ is applied, which resulted in a MDI of 1.7. Unlike a HLR of $0.829 \text{ m}^3/\text{m}^2\text{-h}$, that resulted in a MDI of 4.0, which is not acceptable for plug flow reactors. Short circuits were observed in data collected from the tracer tests performed in the UASB reactor (Figure 3.6). When increasing the HLR in the fixed-film reactor from 0.306 to $10.632 \text{ m}^3/\text{m}^2\text{-h}$ the MDI changed by 0.01 from 1.8 to 1.9. Both MDI values are acceptable by the EPA, who recommends MDI lower than 2, to consider the fixed-film reactor an efficient plug

flow reactor. However, low HLR applied to the fixed-film reactors demonstrated short circuits that may affect the efficiency of the process, as depicted by curves that are not smooth and have points that deviate upward or downward from the curve, (Figure 3.7 (a)). Additionally, high HLR in the fixed-film reactor eliminates short circuits and the capital cost for construction. Nevertheless, the energy cost due to pumping required to recycle the carbon source more often must be evaluated as part of the cost-effectiveness of anaerobic reactors (Figure 3.7). Similarly, when comparing HLR of 0.340 and 12.450 $\text{m}^3/\text{m}^2\text{-h}$ applied to the hybrid reactor, the lowest HLR increases short circuits in the reactor (Figure 3.8 (a)). Also, the MDI was just increased from 2.0 to 2.1, which is still reasonable for plug flow reactors (Figure 3.8). To summarize, the lower the HLR the closer plug flow conditions were approached in the reactors (Table 3.2).

Table 3.2 Summary of hydrodynamics results of high-rate anaerobic reactor

Parameter	High-rate anaerobic reactor					
	UASB		Fixed-film		Hybrid	
HLR ($\text{m}^3/\text{m}^2\text{-h}$)	0.296	0.829	0.306	10.632	0.340	12.450
MDI	1.7	4.0	1.8	1.9	2.0	2.1
HRT (hours)	11.64	3.30	9.9	0.224	9.87	0.235

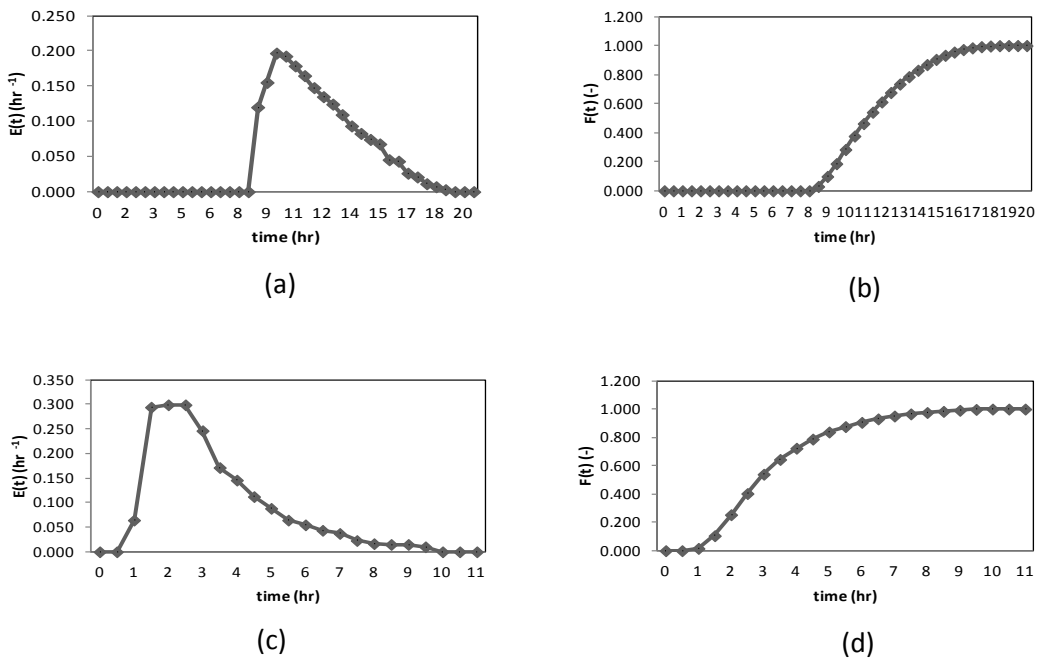


Figure 3.6 Hydrodynamics characteristics of the UASB reactor obtained from tracer tests for $\text{HLR} = 0.296 \text{ m}^3/\text{m}^2\cdot\text{h}$ (a) and (b). and $\text{HLR}=0.829 \text{ m}^3/\text{m}^2\cdot\text{h}$ (c) and (d).

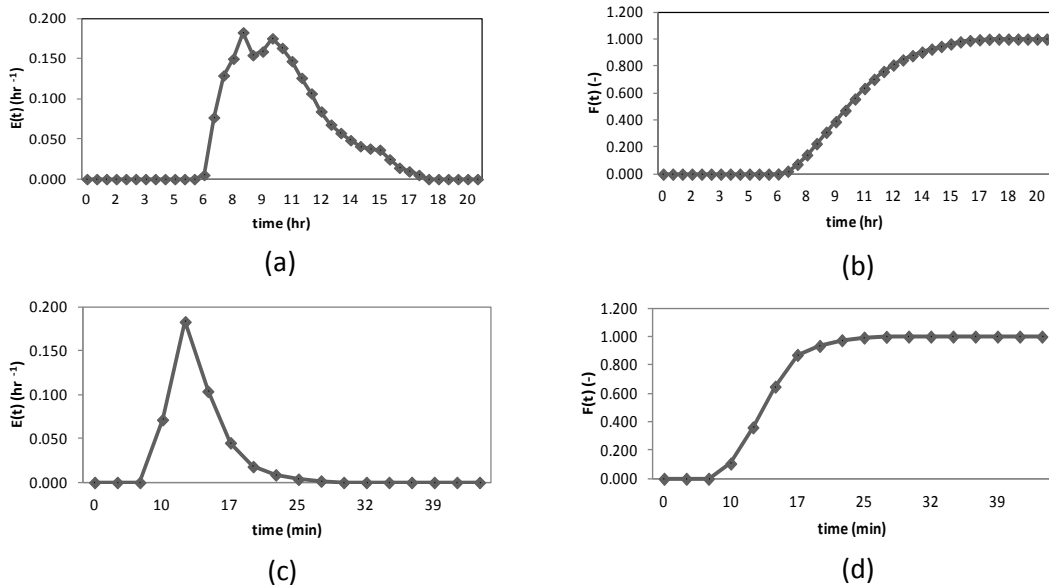


Figure 3.7 Hydrodynamics characteristics of the fixed-film reactor obtained from tracer tests. $\text{HLR} = 0.306 \text{ m}^3/\text{m}^2\cdot\text{h}$ (a) and (b). and $\text{HLR}=10.632 \text{ m}^3/\text{m}^2\cdot\text{h}$ (c) and (d).

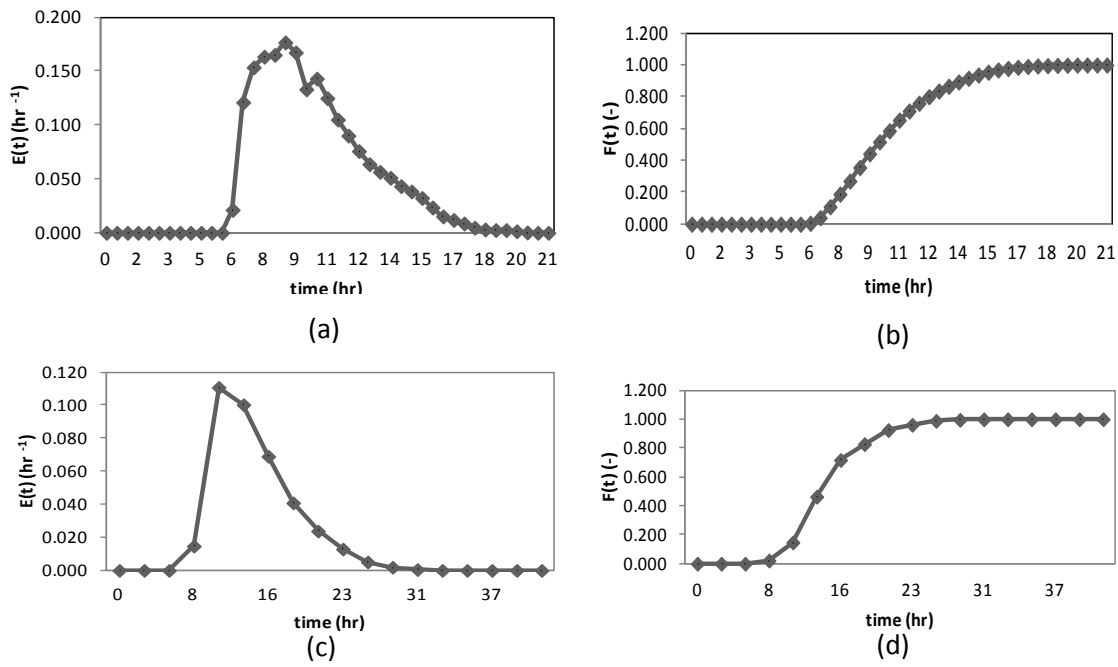


Figure 3.8 Hydrodynamics characteristics of the hybrid reactor obtained from tracer tests.

HLR= $0.340 \text{ m}^3/\text{m}^2\cdot\text{h}$ (a) and (b). and $\text{HLR}=12.450 \text{ m}^3/\text{m}^2\cdot\text{h}$ (c) and (d).

Since no impact in the MDI was observed in the fixed-film and the hybrid reactors, the CFD model was focused on the UASB reactor. The residence time distribution was modeled by the CFD model, which was validated by one of the tracer test. Figure 3.9a shows the cumulative age distribution obtained by the CFD model and the tracer test when a HLR of $0.829 \text{ m}^3/\text{m}^2\cdot\text{h}$ is chosen. Also, a velocity field focused on the section with the highest turbulence is depicted in the Figure 3.9b. Additionally, the average hydraulic retention time and MDI generated by the CFD model are compared (Table 3.3), which reveals a high error in the CFD model of 26% and 42% for the average hydraulic retention time and MDI, respectively. This error is attributable to the inlet configuration of the pilot scale reactor, which was comprised of five different tubes connected to a manifold. However, such inlets are comprised by long tubing that contributes to

supply the tracer unevenly and at different times. Thus, this injection approach altered the dispersion of the tracer in the reactor. A single tubing, where the tracer could be injected, should supply the fluid to each column, thus such tracer can be transported to the reactor evenly. Additionally, the manifold should be installed strictly in the reactor inlet to reduce this source of error.

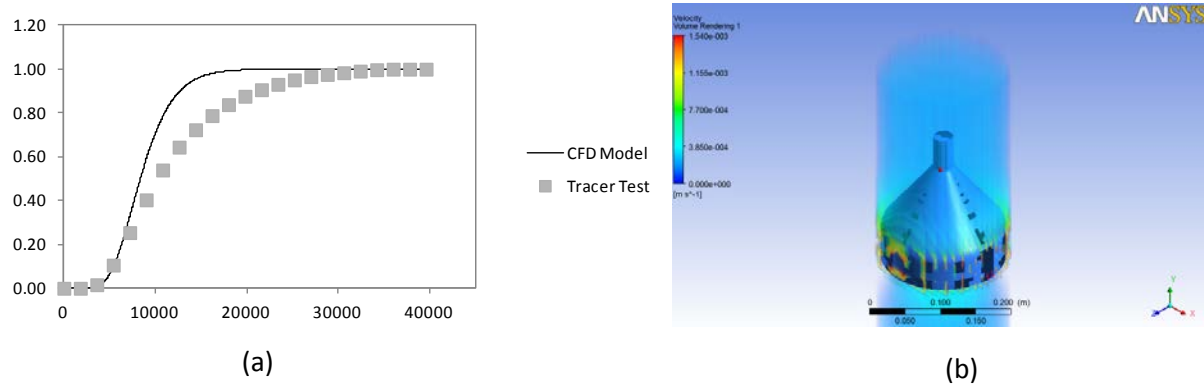


Figure 3.9. (a) Cumulative Age Distribution obtained by CFD model and tracer test at a HLR $0.829 \text{ m}^3/\text{m}^2\cdot\text{h}$ (b) Velocity field in the UASB reactor generated in ANSYS

Table 3.3. CFD model results compared to tracer test

Method	HLR ($\text{m}^3/\text{m}^2\cdot\text{h}$)	Average Retention Time (hr)	MDI
Theoretical	0.829	3.25	-
Tracer Test	0.829	3.30	4.0
CFD Model	0.829	2.45	2.32

3.4 Conclusions

The hydrodynamic characteristics of the fixed-film and hybrid reactor revealed that different HLRs do not impact on the dispersion of the system. The most favorable HLR observed in the UASB reactor, $0.296 \text{ m}^3/\text{m}^2\text{-h}$, is not even suggested in the literature for this reactor configuration where recommended ranges are from 0.70 to $1.5 \text{ m}^3/\text{m}^2\text{-h}$. Additionally, lower HLRs would reduce the need for recirculation pumping, thus contributing to improve the energy efficiency of UASB reactors.

The optimization of the MDI of the fixed-film and hybrid reactors by CFD is not necessary because MDI was not impacted by HLR. However, the MDI of the UASB may be optimized by CFD since the lowest HLR approached an ideal plug flow reactor. The CFD model of the UASB did not capture the real performance of the system due to the influent configuration as mentioned above. Since the tracer results were consistent and the CFD model accomplished the quality requirements in regards with the orthogonality and the skewness, the CFD model suggests that the laboratory conditions of the reactor are creating more dispersion of the tracer, which may have been started at different initial times in real conditions due to an inappropriate design of the inlet through a manifold that is supplying five different tubings inside the reactor (Venayagamoorthy, 2012). As a matter of fact, it is concluded that the inlet should be substituted by a manifold inside the reactor to approach a plug flow reactor.

Chapter 4 SIMULTANEOUS INOCULATION FOR UPFLOW ANAEROBIC SLUDGE BLANKET, FIXED-FILM, AND HYBRID REACTORS

4.1 Introduction

It is stated that the rate at which biomass is accumulated, is governed by the yield (Y) of the substrate to be synthesized (Speece, 2008). Consequently, Speece (2008) claims that anaerobic digestion, which presents lower yields of substrates than the aerobic systems, require longer start-up times. When the Upflow Anaerobic Sludge Blanket (UASB) is to be inoculated, the desired organic loading rate (OLR) is gradually approached to allow microorganisms to be acclimatized (Show et al., 2004). This is accomplished by gradually increasing the flow rate, which consequently increases the operating organic loading rate (Show et al., 2004). As a matter of fact, the Show (2004) increased the OLR of a UASB reactor with synthetic wastewater from 2 g/L-d up to 40 g/ L-d in a maximum period of 135 days. Additionally, it is suggested that a large initial inoculum of granules should be applied to start-up the UASB reactor (Speece, 2008).

On the other hand, when a fixed-film reactor is to be inoculated, a short initial contact between the inoculum and the plastic media is recommended, followed by a constant short hydraulic retention time required to wash out suspended biomass and promote biofilm growth on the plastic media (Escudie et al., 2011). Moreover, Escudie (2011) claimed that only 12 hours of initial contact time was necessary by the microorganisms in a fixed-film reactor to be attached to the carrier particles. Additionally, it was stated that lower hydrodynamics strength during start-up of a fixed-film reactor enhanced the attachment of biomass, whereas a parallel reactor with higher hydrodynamics strength failed during the start-up period (Cresson et al., 2007). Also, Cresson (2007) increased the OLR of the first reactor up to 6 g/L-d after the start-up period was

accomplished, which was the initial set for the second reactor, obtaining successful results regarding the performance of the first reactor.

It is claimed that the packed bed reactor (PBR) has a shorter start-up period compared to the fluidized/expanded and UASB reactors (Speece, 2008). Also, Speece (2008) states that highest efficiencies regarding the retention of inoculum in the reactor of about tenfold could reduce the start-up period up to 80 days, when the retention of inoculum is increased from 100 to 1000 mg/L.

It is important to point out that inoculation for hybrid reactors is not well documented. Moreover, research is necessary when a parallel comparison of high-rate reactors such as the UASB, fixed-film, and a hybrid alternative, need to be inoculated under similar conditions. Therefore, the objective of this research was to integrate the start-up approaches typical for UASB and fixed-film reactors. Consequently, biomass was inoculated in an upflow hybrid reactor prior to the transfer of the inoculated sludge to the UASB, inoculated plastic media to the fixed-film reactor, and both, inoculated sludge and media to a hybrid reactor for the treatment of manure leachate.

4.2 Methods

4.2.1 Inoculation reactor configuration and start-up

The inoculation reactor was built by a 246 liters tank manufactured from medium or high-density polyethylene with U.V. inhibitors, which dimensions are shown in the Figure 4.1. Additionally, the tank was provided on the top by a HDPE pipe of 100 mm, which was intended to reduce the surface area and biogas losses. Moreover, the reactor was kept at about 35 °C by a standard bucket heater and insulation on the bottom and walls to prevent heat losses. Additionally, liquid was supplied to the system using a Geotech Series II peristaltic pump, which is rated at 0 RPM to 350 RPM. Biogas production was measured by the apparatus depicted in Figure 4.3. This

apparatus was comprised by a 18.9 liters polycarbonate water bottle and a 18.9 liters bucket, filled with water, were utilized to estimate volume of biogas production based on liquid displacement in the bottles. Nearly 151.4 liters of plastic media, were placed inside the tank. The system is depicted in Figure 4.3.

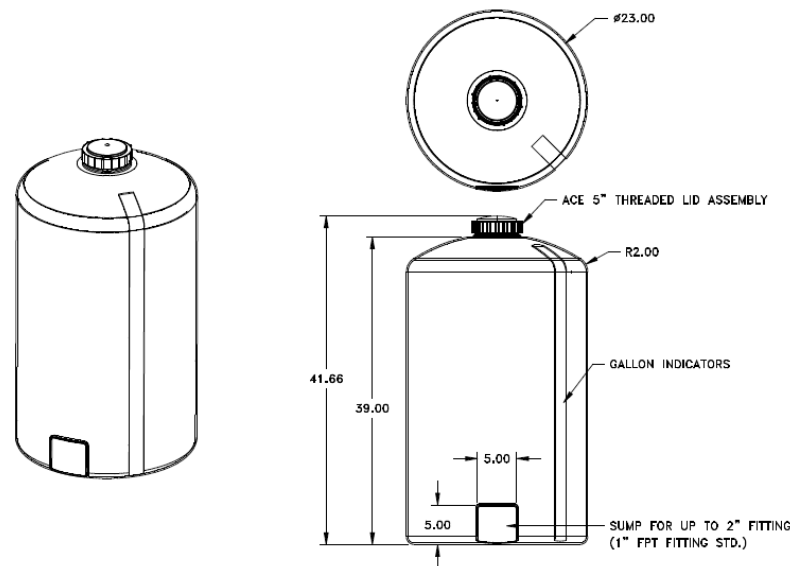


Figure 4.1 Inoculation reactor tank dimensions.

Source: DEN HARTO Industries, Inc.

Table 4.1. Technical specifications of plastic media

Surface area	16.6 m ² /m ³
Cylinder diameter	17.78 mm
Cylinder length	13.97 mm
Weight	136.15 kg/m ³
Specific gravity	0.92 – 0.96
Void space	0.85



Figure 4.2 Plastic media used in inoculation reactor

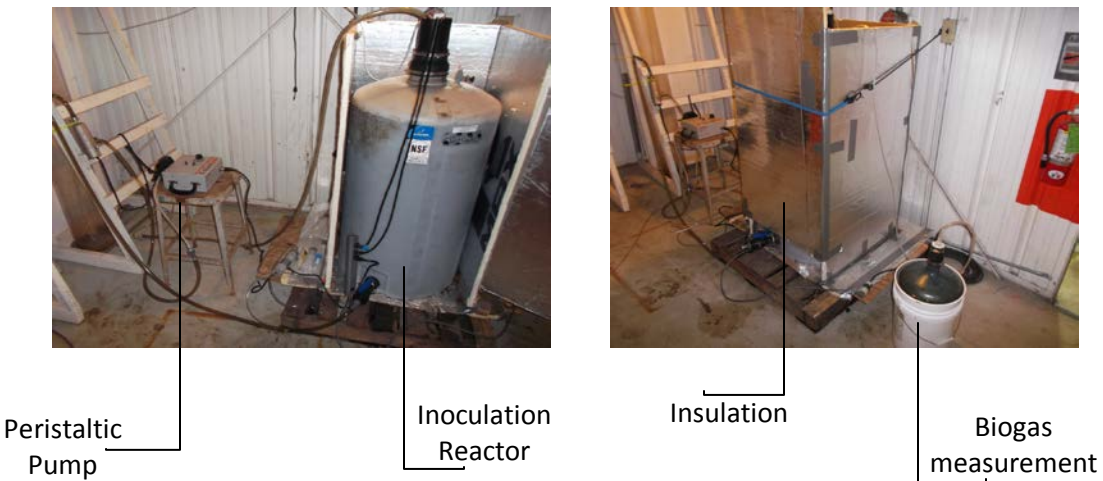


Figure 4.3 Inoculation reactor configuration

The inoculum was provided by an Upflow Anaerobic Sludge Blanket (UASB) reactor of New Belgium Brewing (NBB) located in Fort Collins, CO. The UASB reactor was kept at 37 °C and at a pH of near 7.05 by the time was obtained. According to NBB, the concentration of total solids (TS) and volatile solids (VS) of the provided inoculum was 46.44 g/L and 42.36 g/L, respectively.

Initially, 75.7 liters of inoculum were supplied to the reactor to allow the microorganisms to be in contact with the plastic media while nitrogen gas was supplied to the system in order to promote air stripping. Then, old manure leachate stored from previous research, which contained the stock solution that is typically used for the preparation of defined media in biochemical methane potential assays (Owen et al., 1979), was provided to the system ensure no nutrient limitations during the start-up of the reactor. The nutrients were recycling without adding carbon source for about a day at an upflow velocity of 0.10 m/h in order to maintain a Reynolds number less than 2300, which corresponds to a laminar flow of 0.027 m³/hr. Therefore, turbulence was avoided in the system to promote the attachment of microorganism to the plastic media. Subsequently, 76 g/d and 151 g/d of glucose was supplied to the system at the first and second day, respectively. Then, 151 additional grams of glucose were supplied to the reactor at the third day. As a result, the reactor was operated at organic loading rates of 1 g/L/d and 2 g/L-d. Due to the reduction of pH after glucose was added, before feeding the reactor with manure leachate, the system was supplied by sodium hydroxide (NaOH) until pH was stabilized above 7.

4.2.2 Leach-bed reactor

Since manure leachate was used in further research as a carbon source upon the transfer of the sludge and plastic media to UASB, fixed-film, and hybrid reactors, the inoculation reactor was fed by this substrate in order to acclimatized the microorganisms. Manure provided by JBS Five Rivers Cattle Feeding LLC, located in Greeley, CO., was supplied in 20.3 cm diameter and 43.2 - 76.2 cm length drilled PVC pipes. Additionally, the drilled PVC pipes were located inside a 208.2 liters barrel, which was filled by old manure leachate storage from previous research, containing stock solution used for the preparation of defined media in BMP assays. The leach-bed reactor is depicted in the Figure 3.4. Afterwards, the organic loading rate (OLR) of manure

leachate supplied to the inoculation reactor was gradually increased from 1.4 to 4 g/L-d during nine days. The reactor was operated at an organic loading rate of 4 g/L-d until day 33.



Figure 4.2 leach-bed reactor

4.2.3 Inoculation monitoring and operation

The leach-bed and inoculation reactors were monitored for chemical oxygen demand (COD), temperature, pH, Electrical conductivity (EC), redox potential (pE), percentage of methane in biogas, and cumulative biogas. COD was measured by the 435 COD HR method of the spectrophotometer (Hach DR/2500[®]). The samples were diluted in proportions of 1:10 and 1:100. Afterwards, 2 mL of the diluted samples and a deionized (DI) water sample, used as a control, respectively, were added to the COD digestion reagent vials. The vials were heated at 150 °C during two hours. Then, 20 minutes were waited until reaching about 120 °C. Finally, the vials were transferred to a rack to let them cool down at room temperature and the results were read in the spectrophotometer. The temperature, pH, pE, and EC of the manure leachate and the inoculation reactor were measured by a mercury-free thermometer, AR25 Dual Channel pH/Ion

meter of Fisher Scientific, ORP Testr® 10 (OAKTON), and HI 8733 conductivity meter (HANNA instruments), respectively.

The percentage of methane was initially measured in the Hewlett Packard Series 2180 gas chromatograph, which is equipped with an Alltech column packed with HayeSep Q 80/100 mesh and a thermal conductivity detector. The injector and detector temperatures were both 100 °C and the carrier gas was helium. Calibration curves were done for each test, which presented a minimum R^2 of 0.97. One of the obtained calibration curves is depicted in the Figure 4.2

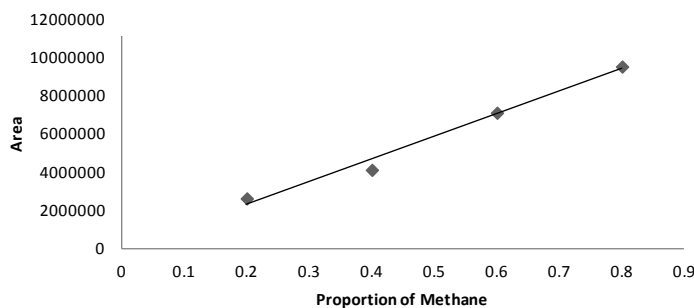


Figure 4.3 Calibration curve of Methane tests in GC ($R^2=0.985$).

In tests that were done later during this research, the carrier gas was depleted and supply issues were encountered in Colorado area. Thus, the methane percentage was determined by injecting a known volume of biogas in a 1N NaOH, the suggested concentration to assess the acetolastic methanogenic biomass (Valcke & Verstraete, 1983). In this method, the carbon dioxide is diluted in the NaOH and the volume of biogas is reduced, which is mainly comprised by methane. The volume difference before and after the injection of biogas in the solution are computed to obtain the percentage of methane out of the biogas.

Last, the cumulative biogas was computed from the measurement device built in the inoculation reactor, which was explained in more detail in section 4.2.1. Additionally, to confirm inoculation of plastic media after startup of the inoculation reactor, samples of plastic media were collected to perform the BMP assay. When the BMP assay was carried out, the plastic media was assumed to be the inoculum, glucose was chosen as the carbon source at concentrations of 0.5, 1, and 2 g/L, and a stock solution for the preparation of defined media was provided (Appendix A), which is used in the BMP assay (Owen et al., 1979). The batch tests were made by syringes and stopcock luer locks (Griffin, 2012). The batch tests were incubated in the Lab-Line Orbit Environ-Shaker at about 37 °C. The batch test with the inoculated plastic media is depicted in the Figure 4.4. After inoculation was accomplished, the inoculated sludge was transferred to an UASB and the bottom part of a hybrid reactor, whereas the inoculated plastic media was transferred to the fixed-film and the upper part of the hybrid reactor mentioned before. The performances of these reactors were compared as described in Chapter 5. No replicates were run in this experiment due to the long time required to select inoculated media from the reactor, which is exposed to high levels of oxygen because it kept open during such task. Moreover, redox potential was slightly elevated on day 18, when the inoculated plastic media was obtained from the reactor (Figure 4.5)



Figure 4.4 Batch test with inoculated plastic media

4.3 Results and Discussion

The inoculation reactor was kept at an average temperature of 37.4 °C (+/- 0.9) during a period of 33 days, where day zero corresponds to first day that manure leachate was supplied. Before this period, the inoculation reactor was fed by glucose (data is provided in Appendix B). The pH was controlled at 7.50 (+/- 0.34). Last but not least, the EC was observed to be 14.2 µS (+/- 1.03) or about 14 mg/L of NaCl, below toxic levels. Regarding inhibition by sodium (Na^+), Speece (2008) states that this cation has been observed to be a problem at 2000 mg/L; however, the methane conversion is gradually inhibited at concentrations of 10,000 mg/L.

The redox potential was maintained below -250 mV (Figure 4.5), which is recommended for anaerobic digestion (Deublein, 2008). The only slight spike was observed after the day 18, when a sample of the plastic media was taken in order to test its inoculation by the biochemical methane potential (BMP) assay.

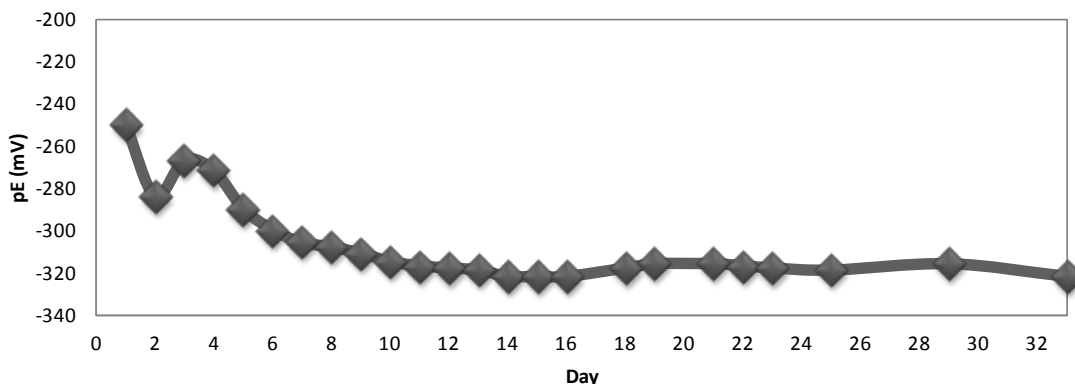


Figure 4.5. Redox potential in the inoculation reactor

Additionally, Figure 4.6 depicts the variation of the percentage of methane produced by the inoculation reactor, which ranged from 45% to 83%. It is important to point out that manure leachate was supplied every four days since the carbon source was being recycled; thus, the

lowest percentages of methane may correspond to the depletion of the carbon source before more was added. The raw data of the inoculation reactor is also shown in the Appendix B.

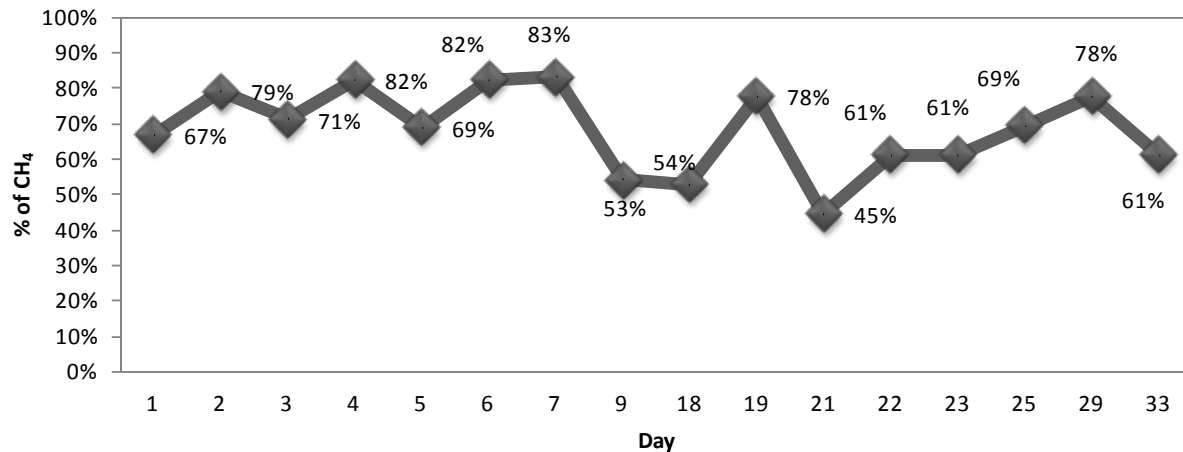


Figure 4.6. Percentage of methane in the inoculation reactor

The BMP results obtained by the inoculated plastic media, which was taken from the inoculation reactor after 18 days. The percentage of methane at a glucose concentration of 0.5 g/L and 1 g/L was 63% (+/- 15%), whereas such percentage was 56% (+/- 22%) at a glucose concentration of 2 g/L. It can be noticed that the highest concentration of glucose, which was 2 g/L, seemed to cause some inhibition during the first four days of the assay; however, this batch test presented the maximal production after 15 days (Figure 4.7). This is the typical behavior of easy degradable substrate (Labatut et al., 2011). However, when calculating the theoretical production of methane from glucose for each concentration described above, it can be noticed that the experimental results reached lower values than the maximal methane potential (Figure 4.8). For instance, the vial with a glucose concentration of 2 g/L achieve 32% (+/- 10%) of the theoretical methane volume, whereas the 1g/L vial reached 31% (+/- 10%) of the theoretical production, and the 0.5 g/L vial accomplished 51% (+/- 22%) of the methane theoretical production. Such

behavior might be attributable to insufficient biomass attached to the plastic media, which is more evident at higher concentrations of glucose. It is recommended that future BMP tests on inoculated plastic media should be carried out in larger test vials to allow more biomass to be supplied, which is attached to the surface of the media but was not measured in this experiment. Last, no replicates were run in this experiment due to the long time required to select inoculated media from the reactor, which is exposed to high levels of oxygen because it kept open during such task. As mentioned before, redox potential was slightly elevated on day 18, when the inoculated plastic media was obtained from the reactor (Figure 4.5).

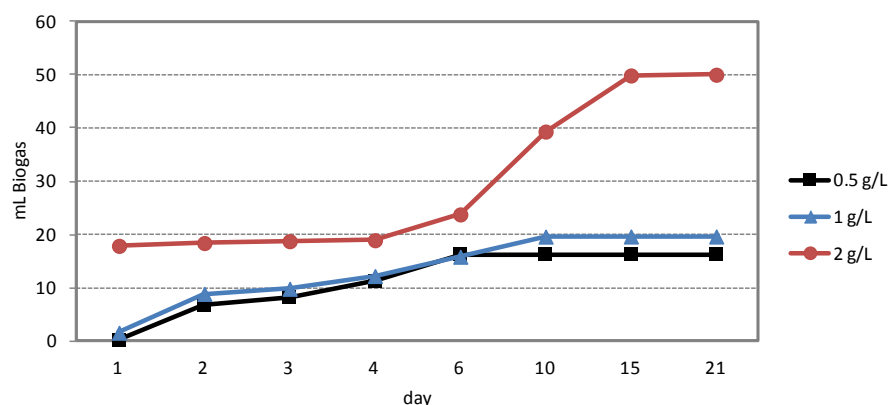


Figure 4.7. Biochemical methane potential of inoculated plastic media.

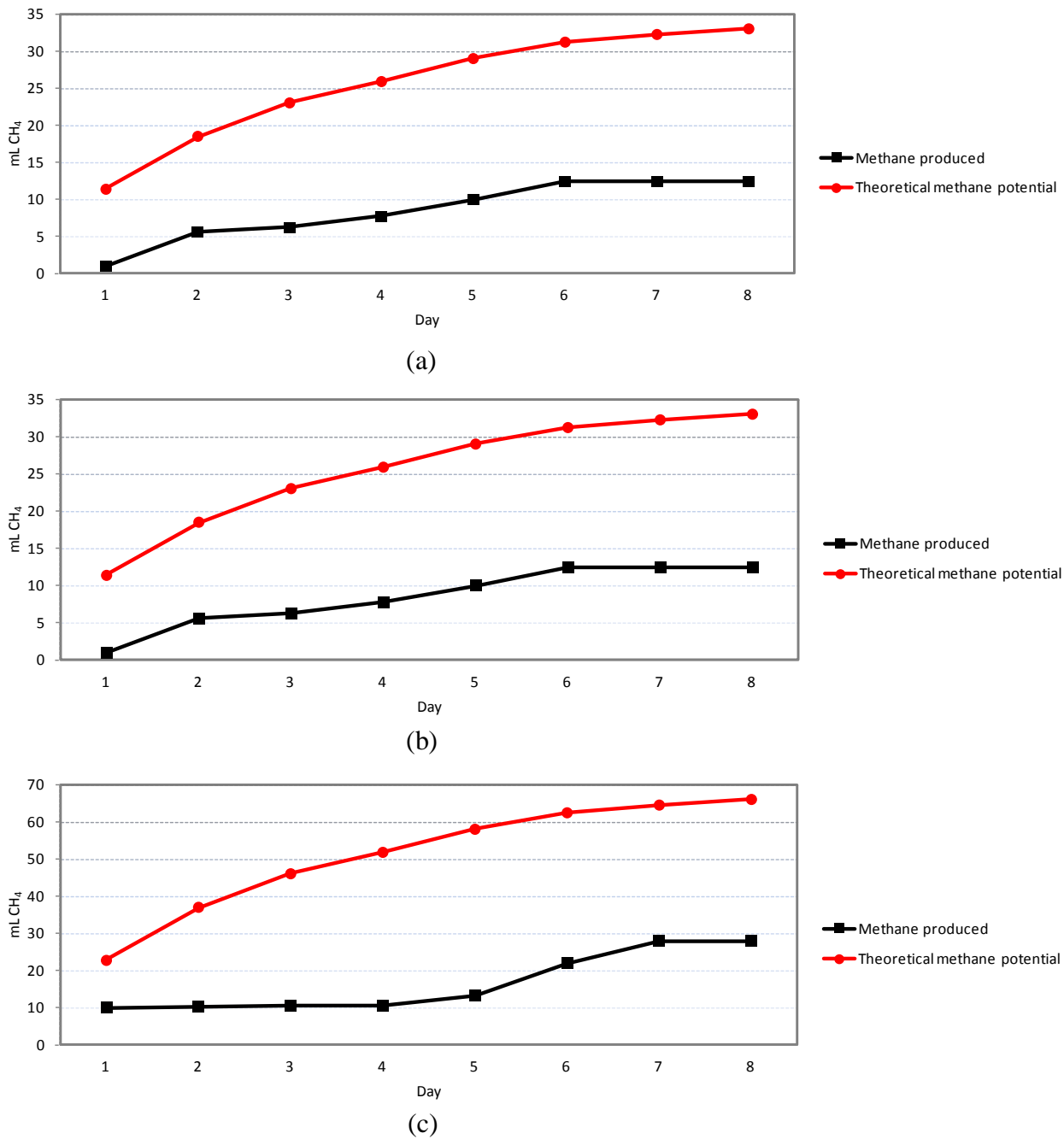


Figure 4.8. Methane produced from inoculated plastic media with respect to the theoretical production. (a) 0.5 g/L of glucose (b) 1 g/L of glucose (c) 2 g/L of glucose

4.4 Conclusions

A simultaneous inoculation of sludge and plastic media prior to the transfer to UASB, fixed-film, and hybrid reactors was proven to be feasible when similar conditions are required for the growth of microorganisms in laboratory scale. Since the OLR is recommended to be maintained steady for the fixed-film reactors, unlike UASB reactors where the OLR is suggested to be gradually increased, the conditions were intended to be ideal for both reactors in this research. In other words, the OLR was gradually increased every four days to promote both, the attachment of microorganisms and the acclimatization of sludge. Laminar flow was maintained at the beginning of the process to avoid turbulence and detachment of microorganisms, and promote settling of sludge. Additionally, large of granules were utilized from a local UASB reactor for the treatment of brewery wastewater, which is recommended for UASB reactors.

Values for redox potential in the inoculation reactor were obtained below -250, which is ideally desired in anaerobic digestion. Additionally, the biogas from the inoculation reactor contained an average percentage of methane of 68% (+/- 12%) during the operation period, reaching a maximum of 83%. The plastic media was proven to be inoculated when BMP assay were carried out at three different concentrations; 0.5, 1, and 2 g/L of glucose. The batch test with the highest concentration of glucose behaved as an easily degradable substrate, with a possible inhibition at the beginning of the process, whereas the lower concentrations behaved as slowly degradable substrates. When computing the theoretical production of methane, it was observed that insufficient biomass was supplied to the experimental BMP test. This is based on lower values of methane for concentrations of glucose of 0.5 g/L, 1 g/L, and 2 g/L, which were 51% (+/- 22%), 31% (+/- 10%), and 32% (+/- 10%), respectively, out of the theoretical methane production from such substrate.

Chapter 5 ANAEROBIC DIGESTION PERFORMANCE OF HIGH-RATE ANAEROBIC REACTORS PROCESSING MANURE LEACHATE

5.1 Introduction

It is stated that the first generation of anaerobic reactors, designed for the treatment of municipal sludge, was the complete stirred tank reactor (CSTR) (Speece, 1983). Recirculation was not implemented in this reactor type, which resulted in the solids retention time to hydraulic retention time ratio (SRT/HRT) of one (Speece, 1983). Tchobanoglous (2003) states that the more popular anaerobic reactors are the batch reactor, CSTR, plug flow reactor (PFR), packed-bed reactor (PBR), and the fluidized-bed reactor (FBR). It is claimed that the most important disadvantage of the CSTR is that high loading rates are only accomplished by very concentrated wastewaters, which reduces the cost-effectiveness of this technology (Rittmann & McCarty, 2001). On the other hand, Rittmann and McCarty (2001) state that operating a PFR under real conditions is not possible, which also requires a very long and thin reactor, and short circuits are inevitable.

The first upflow anaerobic sludge blanket (UASB) was developed by Lettinga in the Netherlands in 1979, which could handle high loading rates up to $30 \text{ kg/m}^3\text{-d}$ (Speece, 1983). At 35°C , an organic volumetric loading rate ranged from 15 to $24 \text{ kg/m}^3\text{-d}$ and a daily average hydraulic retention time (HRT) of 6 hours is recommended (Lettinga, 1991). Also, hydraulic loading rates (HLR) or upflow velocities ranged from 0.7 to 1.5 m/h are typically used (Tchobanoglous, 2003). Last but not least, it is suggested that a large initial inoculum of granules is applied to start-up the UASB reactor (Speece, 2008).

In one of the first studies of upflow packed bed reactors (PBR) in the United States, the packing material was found to have high surface area, and the Reynolds number was kept low to contribute to reduce turbulence in the system and allow settling of unattached microorganisms (Speece, 1983). Also, Speece claims that unattached microorganisms on the packing material as biofilm, are kept in the interstices of the media (1983). This reactor can operate at organic loading ranged from 1 to 6 kg/m³-d (Tchobanoglous, 2003). Tchobanoglous states that The Upflow Attached Growth Anaerobic Expanded Bed Reactor (EBR) is known for having 20% of bed expansion by keeping an upflow HLR of 2 m/h, whereas the Attached Growth Anaerobic Fluidized-Bed Reactor (FBR) requires upflow HLR up to 20 m/h to reach 100% of bed expansion (2003). Additionally, it is stated that the upflow packed reactors have been presented the fastest inoculation among other configurations (Speece, 2008).

The upflow packed-bed anaerobic reactors can be designed as a hybrid configuration, where the upper depth of the column is filled by 50 to 70% of packing material (Tchobanoglous, 2003). Moreover, this configuration can enhance the retention of biomass when the bottom is design unpacked as an UASB, and the top is packed with material (Speece, 2008). In a palm oil wastewater treatment research, an upflow anaerobic sludge-fixed film reactor was fed by organic loading rates from 2.63 to 23.15 g (COD)/L-d getting a methane yield of 0.346 L CH₄/g COD_{removed} (Najafpour et al., 2006).

In the present research, manure leachate was the carbon source to be used. The chemical composition of raw dairy manure has been reported to be 3.5% of VFAs, 5.7% of protein, 16.1% of lipids, 9.6% of hemicelluloses, 32.6% of cellulose, 13.8% of lignin, and a percentage of sugars, starch, and pectin of 16.5% (Labatut et al., 2011). Additionally, Labatut states that the ratio of biochemical oxygen demand (BOD) to the COD (BOD/COD) is 0.47 in manure

separated liquid, whereas this ratio is observed to be 0.36 in raw dairy manure. Moreover, The hydrolysis of cattle manure, measured by VFAs and soluble COD has been proven to be enhanced by 15% and 8%, respectively, when leach-bed reactors are used (Myint & Nirmalakhandan, 2009).

The performance of the UASB, fixed-film, and hybrid reactors, when manure leachate is considered as the carbon source is not well documented. Thus, a review of technologies of these three high-rate reactors is necessary to be developed. This research proposes the design judgments for the anaerobic digestion of manure leachate by such high-rate reactors.

5.2 Methods

5.2.1 Reactor design and configuration

Stability of anaerobic digestion has been compromised by reflocculation or gravity thickening, which are common physical processes observed in suspended growth systems, and turbulence (Speece, 2008). Consequently, inappropriate selection of reactors can result in a poor retention of biomass (Speece, 2008). Speece (2008) states that the favorable conditions to high concentration anaerobic biomass immobilization are fixed surfaces or media that promotes the growing of biomass. Additionally, maintaining high settling rate granules and non-turbulent flows, at the inlets and the upper sections of reactors, contribute to the development of high density biomass (Speece, 2008). Such requirements can be accomplished by the appropriate design parameters for high-rate anaerobic reactors such as hydraulic retention time (HRT), hydraulic loading rate (HLR), and organic loading rate (OLR)) (Table 5.1).

Table 5.1. Design parameters of high-rate anaerobic reactors

High-rate anaerobic reactor	HRT (Hours)	HLR (m ³ /m ² -h)	OLR (kg/m ³ -d)	Recycle ratio
Upflow anaerobic sludge blanket (UASB)	6	0.7 – 1.5	15 – 30	N/A
Upflow packed bed reactors (PBR)	0.5 - 3*	2	1 – 6	0.25 – 5
Fluidized-bed reactor (FBR)	12**	20 – 24	10** - 20	N/A
Hybrid	50	N/A	6	N/A

* Reported values for different industrial wastewaters

**Reported value for glucose

***HLR is not available in the current literature.

N/A: Not data available

It is important to mention that during the inoculation stage of this research, the reactor used for such application was successfully operated at an OLR of 4 kg/m³-d, which is still below the maximal values recommended for high-rate anaerobic reactors. As a result, at this OLR the PFR and hybrid reactors proved to be capable of handling manure leachate without inhibition issues. Additionally, laminar flow, which stated to accomplish at Reynolds numbers below 2000, was guaranteed during the inoculation stage as recommended by literature. However, when the inoculum was transferred to the high-rate reactors of this research, the outlet configuration of such reactors promoted turbulent flows that are not suitable to maintain high-density biomass (Speece, 2008). This issue is caused by the small diameter outlets, which are increasing the Reynolds numbers above 4000.

The reactors were made by acrylic with dimensions of 2.19 meters of length and a cross section area of 289.5 cm² (Figure 5.1 (a)). Inside-of-pipe grippers made with glass-reinforced ABS plastic and a diameter of 19 cm were used to adapt an influent and effluent to the columns (Figure 5.1 (b)). The grippers (Figure 5.1 (c)) are equipped by large zinc wing nut, natural rubber o-ring, and galvanized carriage bolt to prevent corrosion. The gripper mass is 1.37 kg and is capable to handle up to 12 meters of back pressure. Five 3.2 mm diameter holes were drilled in the influent gripper, while ten 6.4 mm holes were drilled in the effluent. The inlet and outlet were provided by hose bars and vinyl tubing. Also, a HDPE funnel was used to emulate the gas collection system. The fixed-film and hybrid reactors configurations were also provided by plastic media. 1.83 meters of depth was filled by plastic media in the fixed film reactor, whereas the upper section of the hybrid reactor was filled by 0.64 meters of plastic media. The media was provided by Entex Technologies Inc, which technical specifications are described in the Table 5.2. The reactors configurations and the plastic media are depicted in the Figures 5.1 and 5.2, respectively.

Table 5.2. Technical specifications of plastic media

Surface area	16.6 m ² /m ³
Cylinder diameter	17.78 mm
Cylinder length	13.97 mm
Weight	136.15 kg/m ³
Specific gravity	0.92 – 0.96
Void space	0.85

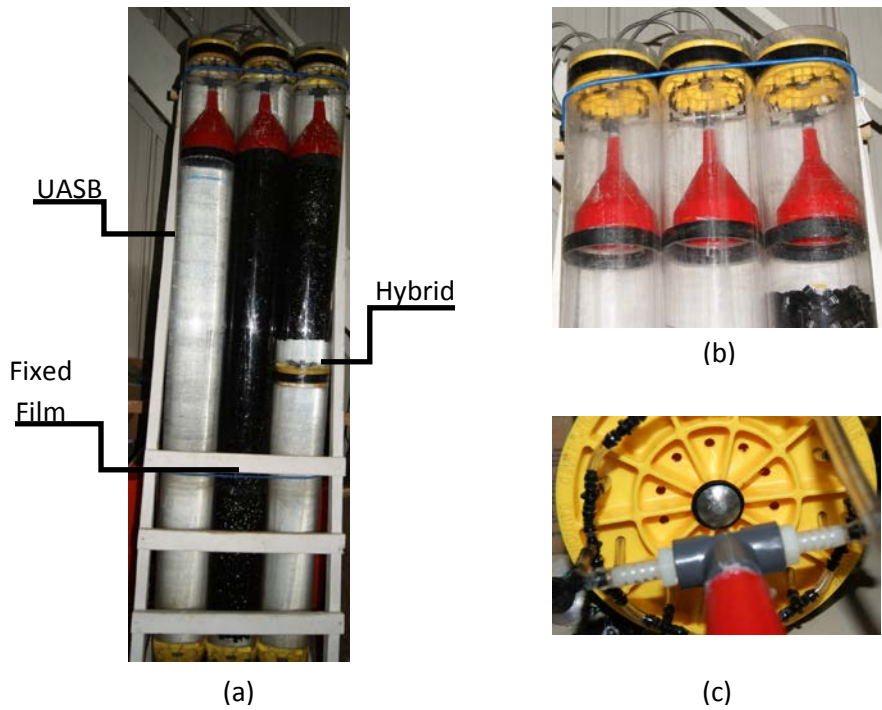


Figure 5.1 (a) Anaerobic reactors (b) Gas collection system (c) Effluent



Figure 5.2 Plastic media used in the fixed-film and hybrid reactors

Liquid was supplied to the reactors with a peristaltic pump Master Flex I/P Model 77600-62 and a high capacity pump controller model 7591-60. Manure leachate was chosen as a carbon source. The high-rate reactors in operation, the heating and insulation system, the gas-liquid separation, and the gas measurement device are depicted in the Figure 5.3. The depicted gas-liquid

separation system, was implemented in this research after a vacuum was observed in the system. To avoid turbulent flows in the system described above, the actual pressurized gripper and the small diameter outlets should be replaced by an open-channel system instead that guarantees a laminar flow.

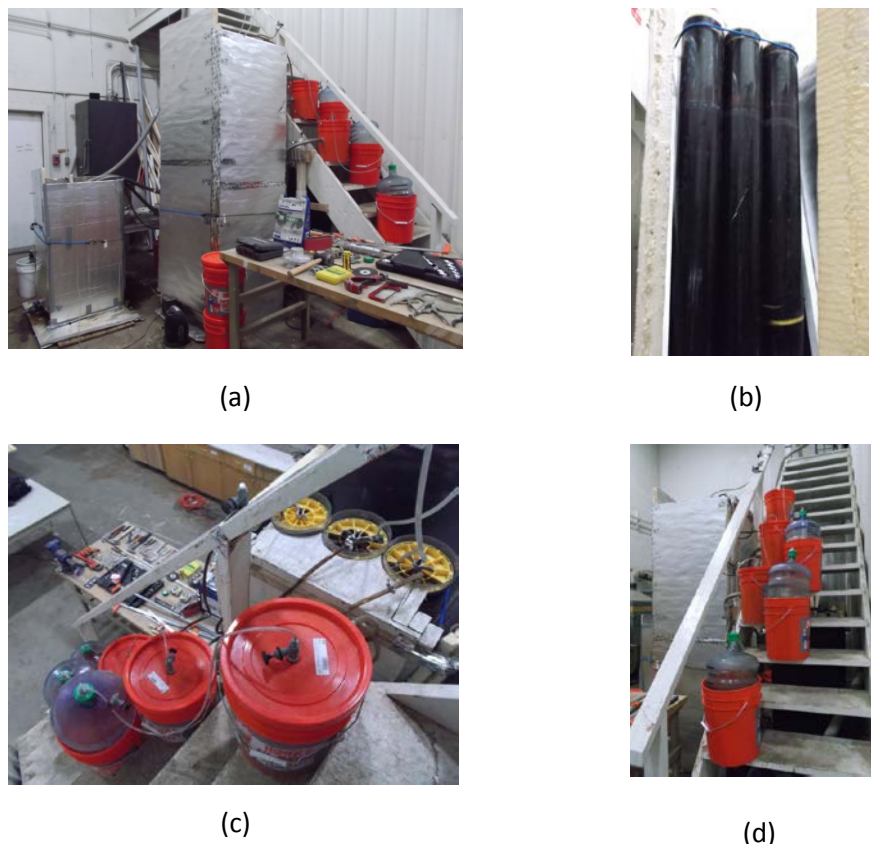


Figure 5.2 (a) Heating and Insulation (b) High-rates reactors fed by manure leachate (c) Gas-liquid separation (d) Gas measurement

Due to limitations of the available peristaltic pump for this research, which presented a short lifetime of its tubing when using high flow rates, the minimum flow rates capable to supply manure leachate to the three reactors were set. The organic loading rates were computed by

dividing the average chemical oxygen demand (COD) concentration, which was found to be 3,833 mg/L (+/- 2,317) by the average hydraulic retention time (Table 5.3).

Table 5.3. Operational parameters of the high-rate anaerobic reactors

Parameter	UASB	Fixed film	Hybrid
Flow rate (L/day)	8.6	8.9	9.9
HLR ($m^3/m^2\text{-h}$)	0.296	0.306	0.340
HRT (days)	11.64	9.90	9.87
OLR ($kg/m^3\text{-day}$)	7.90	9.29	9.32

5.2.2 Performance monitoring and operation of anaerobic reactors

The methods applied for the monitoring and the operation of the high-rate anaerobic reactors are described below. Parameters such as the solids retention time (SRT), chemical oxygen demand (COD), and ammonia have been recommended in this research; however, the SRTs for each reactor were not conducted due to experimental setup problems that will be described. The COD and ammonia values are depicted in the results, where operational issues were observed. Additionally, a new method for analyzing volatile fatty acids (VFA) by mass spectrometry has been developed in this research. Additionally, the solids retention time, also known as cell residence time, should be measured for its later calculation by the Equation 5.1 due to the relevance of this parameter regarding the efficiency and operation of the anaerobic digestion (McCarty, 1964a).

$$SRT = \frac{M_t}{M_e} \quad \text{Equation 5.1}$$

Where:

SRT = Solids retention time

M_t = Total weight of suspended solids in treatment system

M_e = Total weight of suspended solids leaving the system per day, including both the deliberately wasted and that passing out with the plant effluent

The parameters used for the monitoring and operation of the influent and the UASB, fixed-film and hybrid reactors were the chemical oxygen demand (COD), temperature, pH, Electrical conductivity (EC), redox potential (pE), percentage of methane, and cumulative biogas. The COD of the manure leachate was measured in the DR/2500 spectrophotometer of HACH®. The samples were diluted in proportions of 1:10 and 1:100. Afterwards, 2 mL of the diluted samples and a deionized (DI) water sample, used as a control, respectively, were added to the COD digestion reagent vials. The vials were heated at 150 °C during two hours. Then, 20 minutes were waited until reaching about 120 °C. Finally, the vials were transferred to a rack to let them cool down at room temperature and the results are read by the 435 COD HR method of the spectrophotometer. The temperature, pH, pE, and EC of the manure leachate and inoculation reactor were measured by a mercury-free thermometer, AR25 Dual Channel pH/Ion meter of Fisher Scientific, ORP Testr® 10, and HI 8733 conductivity meter, respectively. Additionally, the AR25 Dual Channel pH/Ion meter of Fisher Scientific was used to measured ammonia. Calibration curves were developed for each test, which presented a minimal R^2 of 0.8652. One calibration test of the ammonia test is shown in the Figure 5.3.

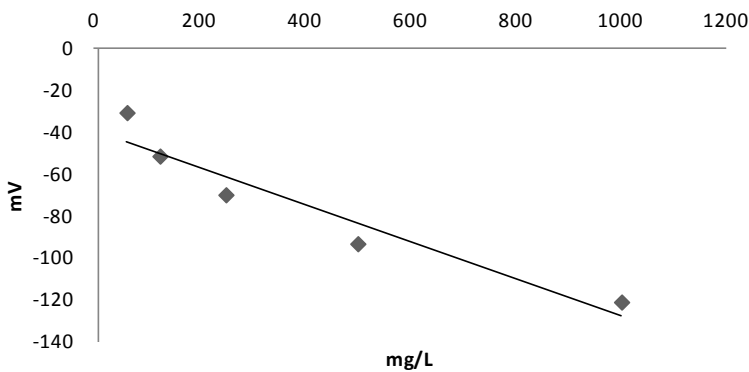


Figure 5.3 Calibration curve of Ammonia Test ($R^2=0.9175$)

Total suspended solids (TSS) is measured as the portion retained out of a sample of 0.5 mL on the Millipore glass fibre prefilter ranged from 0.2 to 0.60 μm , which was vacuumed and later dried out at 110 °C by the Thermo Scientific Model 6547. Additionally, the volatile suspended solids (VSS) is measured after the portion of TSS is ignited at 550 °C in the Thermo Scientific Lindberg Blue M.

The percentage of methane was measured in the Hewlett Packard Series 2180 gas chromatograph, which is equipped with an Alltech column packed with HayeSep Q 80/100 mesh and a thermal conductivity detector. The injector and detector temperatures were both 100 °C and the carrier gas was helium. The cumulative biogas was computed by the data obtained from the measurement device shown in the Figure 5.2d.

5.2.3 Calibration and determination of Volatile Fatty Acids (VFAs) in sludge and manure leachate by Mass Spectrometry

Gas chromatography (GC) is claimed to be the most accurate method to measure volatile fatty acids (VFAs) (Siedlecka et al., 2008). The main steps involving the calibration and determination

of VFAs in aqueous samples and waste are the acidification, extraction, and derivatization (Manni, 1995; Siedlecka et al., 2008). Various experiments were carried out during this research to develop a protocol regarding the determination of VFAs by GC; however, numerous by-products generated after the derivation was accomplished, which made the experiment difficult to develop by GC. Thus, the samples that were obtained after the extraction and derivatization approaches reported in the literature were analyzed by mass spectrometry (MS), which made feasible the identification of VFAs of interest in environmental engineering.

Initially, the samples are acidified at a pH of 2 by either nitric or sulfuric acid, which selection was reported to be irrelevant in the accuracy of the test (Manni, 1995). Afterwards, the extraction was accomplished by adding an equal volume of Diethyl Ether to the sample (Manni, 1995; Siedlecka et al., 2008). The sample is recommended to be shaked by 10 minutes (Siedlecka et al., 2008); however, 1 minute was observed in this research to be enough to obtain the ether phase. Then, a small amount of Na₂SO₄ is added to the ether phase to absorb traces of water (Manni, 1995). Finally, 500 µL are transferred to GC vials, where the derivatization is completed by adding 150 µL of diazomethane (Siedlecka et al., 2008). Moreover, Trimethylsilyldiazomethane (2M solution in diethyl ether) was successfully used as a derivatization reagent in this research. As a matter of fact, it is claimed that this relatively new derivatization reagent has been successfully used for this and other applications such as the determination of pharmaceuticals (Siedlecka & Kumirska, 2012). The samples of VFAs obtained from the extraction and derivation approach, were analyzed in the Agilent 5973 Network Mass Selective Detector. The apparatus is equipped with a MS detector. The column used was a Rtx-624Sil MS, 30 m length, 0.25 mm ID, and 1.4 um film thickness. The carrier gas was helium. The temperature program

was 40 °C for 2 minutes and a linear gradient from 40 to 100 °C at 10 °C min⁻¹ and from 100 to 280 °C at 30 °C min⁻¹.

Calibration curves of the VFAs of most interest in anaerobic digestion were performed in this research due to its importance in the hydrolysis stage (O'Rourke, 1968) and inhibition of microorganisms (Deublein, 2008). These VFAs are formic, acetic, propionic, N-butyric, Iso-butyric, N-valeric, and Iso-valeric acids. Additionally, the assay was tested on municipal sludge provided by the Drake Water Reclamation Facility of Fort Collins, CO. since fresh manure leachate was not available by the time the test was accomplished. The results are shown in table 5.4. The calibration curves of the VFAs are depicted in the Figure 5.4.

Table 5.4. Test of the VFAs assay by MS in the Sludge of Drake Water Reclamation Facility of Fort Collins, CO.

Sample Description	Area*			Concentration (mg/L)		
	Formic	Acetic	Propionic	Formic	Acetic	Propionic
Sludge inside the digester	432650	1199814	11882225	243	118	197
Influent sludge of digester	131967	1722911	273319	74	170	19

*Not measurable values of butyric and valeric acid were found

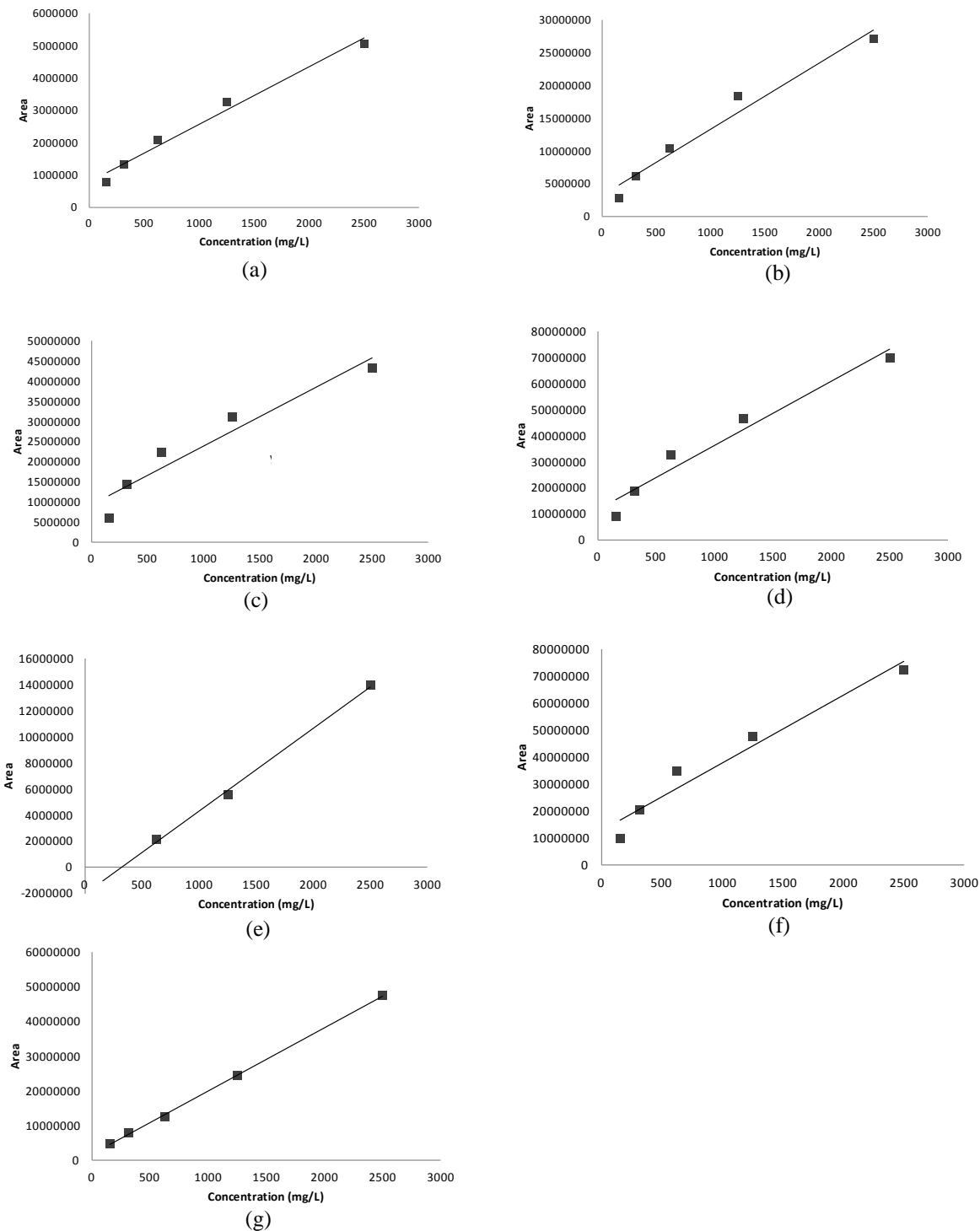


Figure 5.3 Calibration curves of VFAs analysis by MS (a) Formic acid ($R^2=0.9827$) (b) Acetic acid ($R^2=0.9657$) (c) Propionic Acid ($R^2=0.9237$) (d) N-butyric acid ($R^2=0.9551$) (e) Iso-Butyric acid ($R^2=0.9978$) (f) N-valeric acid ($R^2=0.9543$) (g) Iso-valeric acid ($R^2=0.9993$)

5.3 Results and Discussion

The results obtained in this research, start upon inoculated sludge and plastic media from a previous research (Chapter 4) were transfer to the UASB, fixed-film, and hybrid reactors studied here. Low temperatures were encountered when the transferring was carried out (Figure 5.4). This issue was controlled by heaters and insulation of the reactors. Additionally, an unusual behavior of the pH was observed (Figure 5.5), which is usually required to be controlled due to the production of organic acids (McCarty, 1964b).

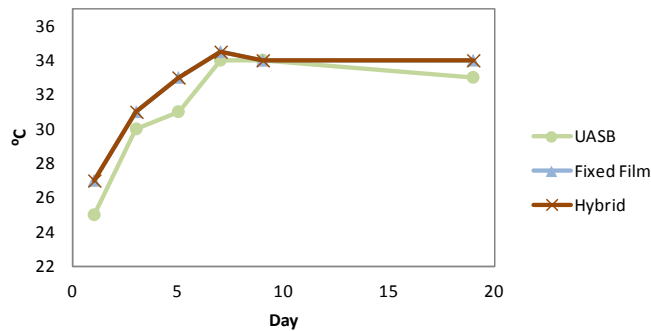


Figure 5.4. Effluent temperature of high-rate anaerobic reactors

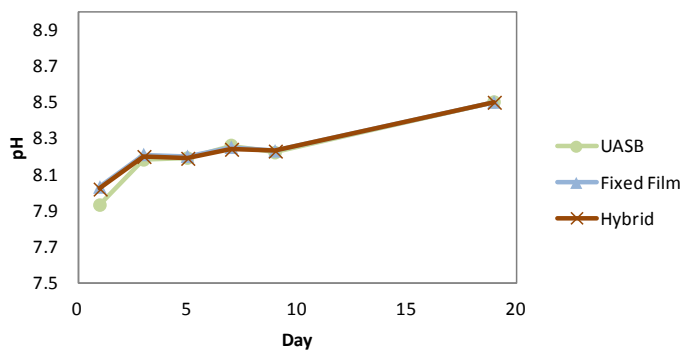


Figure 5.5. Effluent pH in high-rate anaerobic reactors

Also, the percentage of COD removal dropped consistently in all the reactors (Figure 5.6). Ammonia concentration stayed below toxic levels (Figure 5.7), such levels are stated at concentrations above 3000 mg/L (McCarty, 1964c). Total suspended solids (TSS), and volatile suspended solids (VSS) values were also dropped in the reactors effluent (Figure 5.8).

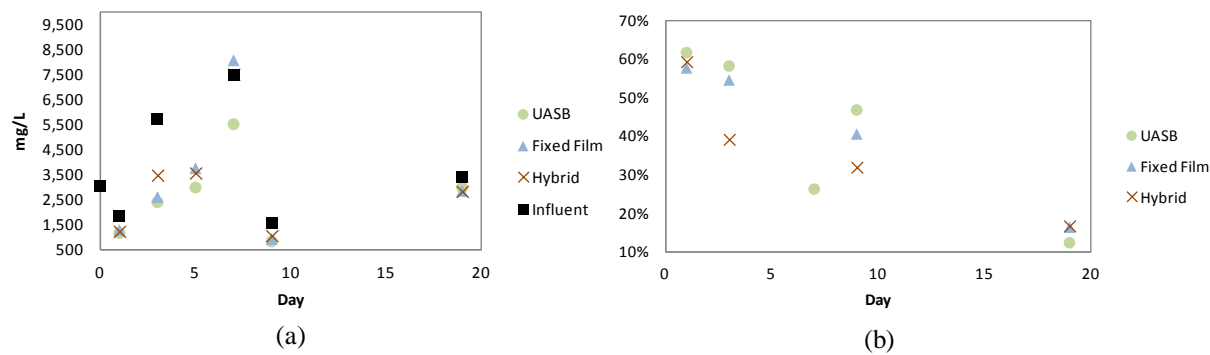


Figure 5.6. Influent and Effluent COD in high-rate anaerobic reactors (a) COD concentration (b) % of COD removal

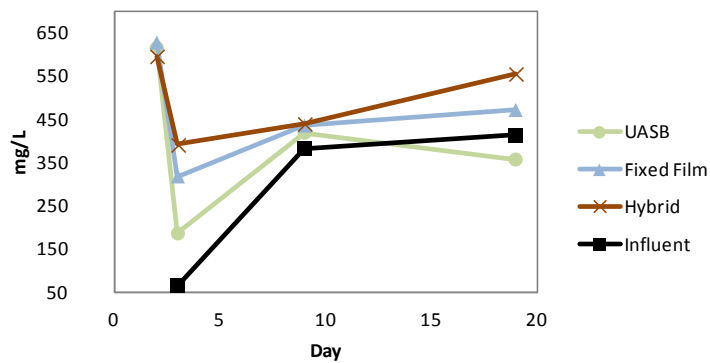


Figure 5.7. Ammonia monitoring in high-rate reactors

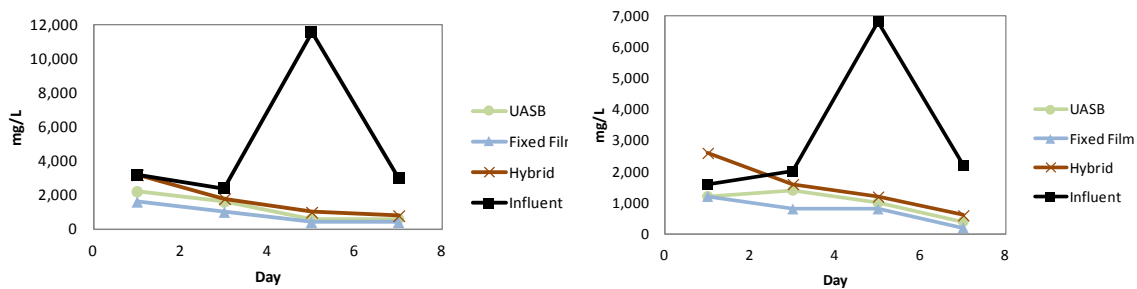


Figure 5.8. TSS and VSS monitoring in high rate reactors

Last, redox potential behaved as expected in these reactors by reaching values below -250 mV (Figure 5.9), which is suggested for anaerobic digestion (Deublein, 2008). However, positive redox values were observed after the eighth day, which was initially thought to be caused by an error in the apparatus used for the measurement. Nevertheless, turbulence was observed in the effluent, which was thought to be cause of this trend. After this issue was found, a new gas-liquid separation device (Figure 5.2) was implemented, which fixed the problem for a short time but the redox potential was gradually depleted by the time this research was written. It is believed that air was entering the reactor systems, preventing the ability to achieve completely anaerobic conditions.

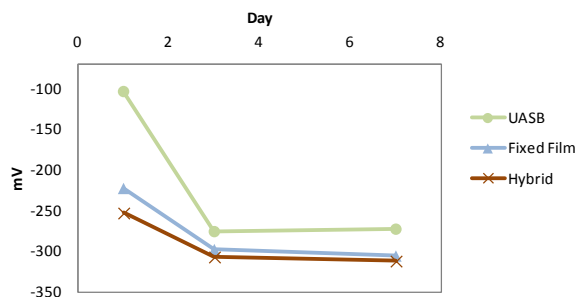


Figure 5.9. Effluent redox potential in high rate reactors

5.2 Conclusions

Since anaerobic conditions could not be accomplished in the high-rate reactors described above, recommendations to enhance the experiment design are provided in Chapter 6, where some of the observed issues such as oxygen intrusion, turbulence, and designed parameters are addressed. The Volatile fatty acids (VFAs) test developed for this research will be of significant contribution in the anaerobic digestion of manure leachate, which can be used in future work for the improvement of hydrolysis and detection of inhibitors compounds.

Chapter 6 CONCEPT DESIGN OF HIGH-RATE ANAEROBIC REACTORS TO PROCESS MANURE LEACHATE AT A PILOT SCALE

6.1 Introduction

It has been demonstrated in previous research, stated in Chapter 4, that manure leachate could be digested in a hybrid inoculation anaerobic reactor at an organic loading rate (OLR) of $4 \text{ kg/m}^3\text{-d}$. Additionally, tracer tests were conducted, as depicted in Chapter 3, on high-rate anaerobic reactors such as the UASB, fixed-film, and a hybrid alternative. This research, performed at a pilot scale, showed how plug flow conditions were approached as the HLR was reduced.

On the other hand, when the inoculated sludge and media by manure leachate was transferred to the high-rate anaerobic reactors, digestion was unsuccessful. This might be attributable to several issues such as oxygen intrusion, development of a turbulent flow, and design judgments. It was claimed in Chapter 4 that turbulent flows at the inlet and outlet of reactors are unsuitable to maintain high-density biomass in the reactors. Moreover, it was demonstrated in Chapter 3 that the actual inlet configuration, comprised by five tubings, leads to an unevenly supply of the tracer since the manifold was not installed inside the reactor, which provided a source of error when comparing the results with a computation fluid dynamic (CFD) model.

Due to the above, this chapter has focused on providing the amendments to enhance the actual columns used to emulate the high-rate anaerobic reactors. Moreover, the present chapter establishes the experiment design of these reactors such as the hydraulic retention times (HRT), organic loading rates (OLR), and the recycled rates based on the hydraulic loading rates (HLR).

6.2 Methods

6.2.1 Design parameters

In this chapter, the average chemical oxygen demand (COD) of manure leachate computed from the data depicted in Appendix B will be taken into account for the experiment design. Such COD concentration was found to be 26.58 kg/m^3 (± 16.12). Also, despite that an OLR of $4 \text{ kg/m}^3\text{-d}$ was proven to be feasible for digestion of manure leachate, this is yet lower than the recommended OLRs for UASB, FBR, and hybrid reactors (Table 6.1). The high-rate reactors previously described in sections 4.2.1 and 5.2.1 will be applied in the new experiment. The net volumes of such reactors are 78, 68, and 65 liters for the UASB, fixed-film, and hybrid reactors, respectively, and the cross section area of all the reactors is 0.029 m^2 .

The hydrodynamics researched for the high-rate anaerobic reactors will be taken into account for the experiment design (Table 6.2). Since a low HLR applied to the UASB reactor turned out to approach plug flow conditions without short circuits issues as stated in Chapter 3 (Section 3.3), $0.3 \text{ m}^3/\text{m}^2\text{-h}$ was selected for the design value. On the other hand, because low HLRs applied to the fixed-film and hybrid reactors resulted in some short circuiting and notable differences were not observed on the MDI at high HLRs, these reactors will be design at $10.6 \text{ m}^3/\text{m}^2\text{-h}$ and $12.5 \text{ m}^3/\text{m}^2\text{-h}$, respectively. By considering the above information, the OLR can be computed by taken into account the flow rate, COD concentration, and volume of the reactor (Equation 6.1).

Table 6.1. Design parameters of high-rate anaerobic reactors (Tchobanoglous, 2003)

High-rate anaerobic reactor	OLR ($\text{kg/m}^3\text{-d}$)
Upflow anaerobic sludge blanket (UASB)	15 – 30
Upflow packed bed reactors (PBR)	1 – 6
Fluidized-bed reactor (FBR)	10* - 20
Hybrid	6

*Reported value for glucose

Table 6.2 Summary of hydrodynamics results of high-rate anaerobic reactor

Parameter	High-rate anaerobic reactor					
	UASB		Fixed-film		Hybrid	
HLR ($\text{m}^3/\text{m}^2\text{-h}$)	0.296	0.829	0.306	10.632	0.340	12.450
MDI	1.7	4.0	1.8	1.9	2.0	2.1

$$OLR = \frac{COD}{HRT} \quad \text{Equation 6.1}$$

Where:

OLR = Organic loading rate, $\text{kg/m}^3\text{-d}$

COD = Chemical oxygen demand concentration, kg/m^3

HRT = Hydraulic retention time, hours

The required flow rate for each high-rate anaerobic reactor were computed by taking into account the recommended OLR values and the COD concentrations of manure leachate obtained during the inoculation stage (Table 6.3). The recycle flows and ratios are consequently calculated by taking into account the researched HLRs (Equation 6.2) and the required flow rates (Table 6.4).

$$HLR = \frac{Q_{in} + Q_R}{A} \quad \text{Equation 6.2}$$

Where:

HLR = Hydraulic loading rate, $\text{m}^3/\text{m}^2\text{-h}$

Q_{in} = Inlet flow rate, m^3/h

Q_R = Recycle flow, m^3/h

A = Cross section area

Table 6.3 Required flow rates to achieve the recommended OLRs

Parameter	UASB		Fixed-film		Hybrid
Required OLR ($\text{kg}/\text{m}^3\text{-d}$)	15	30	6	20	6
Reactor volume (m^3)	0.078		0.068		0.075
COD concentration (kg/m^3)	26.6	26.6	26.6	26.6	26.6
Feed flow rate (L/d)	44.0	88.0	15.4	51.2	16.9
HRT (d)	1.77	0.89	4.43	1.33	4.43

Table 6.4 Required recycle flows and ratios to achieve the researched HLRs

Parameter	UASB		Fixed-film		Hybrid
Researched HLR ($\text{m}^3/\text{m}^2\cdot\text{h}$)	0.296		10.632		12.450
Feed flow rate (L/d)	44.0	88.0	15.14	51.2	16.9
Required Recycle flow (L/d)	6.7	4.9	307.7	306.2	360.3
Recycle Ratio	0.15	0.06	20.04	5.98	21.28

6.2.2 Inlet - Outlet & Gas Collection Setup

As mentioned in previous chapters, the multi-stage anaerobic digestion (MSAD) process is comprised by the leach-bed reactor, where the manure leachate is obtained, followed by the manure leachate storage tank, and the high-rate anaerobic reactor. Also, control valves are strategically located in the system to ease the operation of reactors, and maintenance of pipes and pumps when required (Figure 6.1). The researched high-rate anaerobic reactors such as the UASB, the fixed-film, and the hybrid will be configured as detailed in previous chapters. Nevertheless, since the previous setup contributed to develop a turbulent flow at the outlets and supply the tracer unevenly at the inlets, such devices are recommended to be modified (Figure 6.2). The inlet should be replaced by a manifold comprised by a PVC pipe crossing the column, which will allow that the injected tracer in such pipe is distributed simultaneously in the reactor. Additionally, to avoid turbulence at the outlet of the reactors, the actual pressurized system must be replaced by either a crossing PVC pipe and a 90° elbow facing upwards or a surrounding weir made by acrylic, which is the same material used for the columns. Also, this outlet setup will facilitate the gas-liquid separation in the reactor, thus the biogas can be collected in a manifold located at the top of the columns, which could be also made by PVC pipe. The biogas volume measurement will be configured as detailed in sections 4.2.1 and 5.2.1 of chapters 4 and 5, respectively.

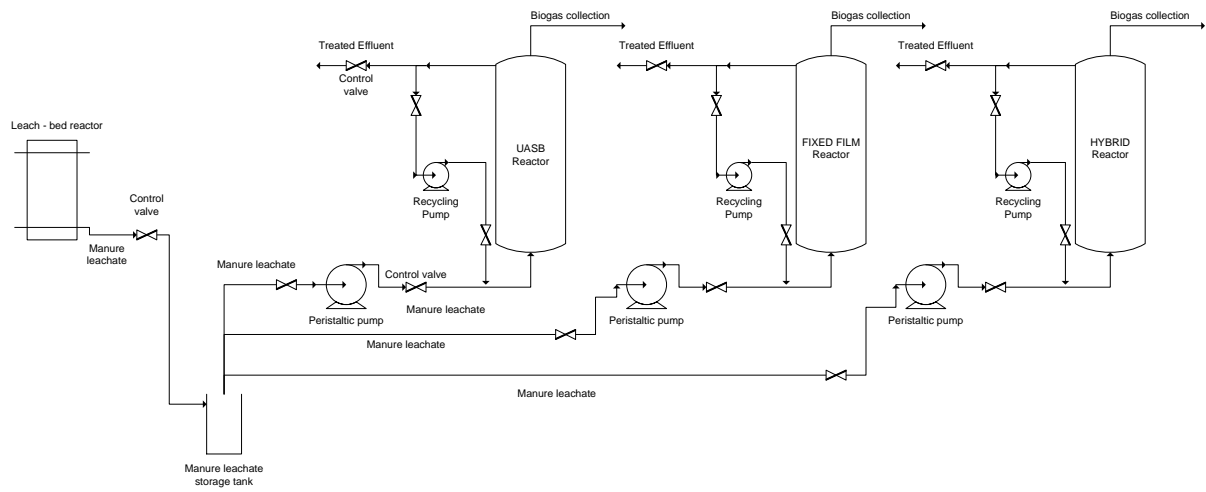


Figure 6.1 High-rate reactors configuration

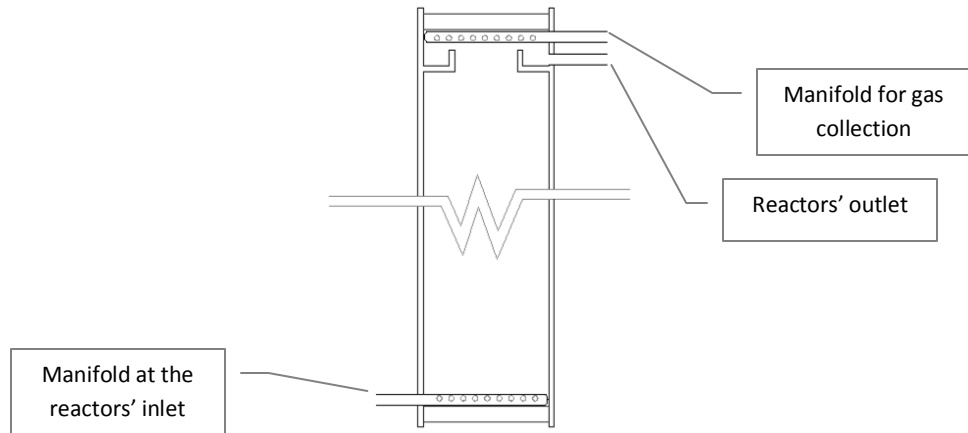


Figure 6.2 Inlet & Outlet configuration of columns

Profile view

6.2.3 Monitoring

The analytical parameters recommended for this research have extensively been described in previous chapters and detailed in chapter five. Such parameters and their standard operating procedures are summarized in this chapter for monitoring purposes in future research (Table 6.5).

Table 6.5 Sampling locations and methods

Sampling Locations	Analytical Parameter	Standard Operating Procedures (SOP)	Sample Volume
Leach-bed reactor Reactors' outlet	COD	Spectrophotometer 435 COD HR method HACH®	0.5 – 2 mL
Leach-bed reactor Reactors' outlet	Fatty acids	Mass spectrometry (MS)	50 mL
Leach-bed reactor Reactors' outlet	Methanogenic activity	Bioassay for monitoring biochemical methane potential and anaerobic toxicity	100 mL
Leach-bed reactor Reactors' outlet	pH	AR25 Dual Channel pH/Ion meter Fisher Scientific	50 mL
Leach-bed reactor Reactors' outlet	TSS / VSS	Thermo Scientific Model 6547 Thermo Scientific Lindberg Blue M	0.5 mL
Leach-bed reactor Reactors' outlet	EC	HI 8733 conductivity meter	50 mL
Reactors' outlet	Temperature	Mercury-free thermometer	100 mL
Reactors' outlet	Redox potential	ORP Testr® 10	100 mL
Reactors' inlet and outlet	Ammonia	AR25 Dual Channel pH/Ion meter Fisher Scientific	50 mL
Reactor's gas collection	CH ₄ , CO ₂	Gas chromatography	20 uL

Chapter 7 CONCLUSIONS

Hydrodynamics characterization of high-rate reactors revealed that variations in the hydraulic loading rates (HLR) did not make substantial impact in the Morrill Dispersion Index (MDI) of the fixed-film and hybrid reactors. These two reactors maintained plug flow reactors conditions when HLR was changed. On the other hand, the MDI of the UASB reactor was impacted when different HLRs were applied. As a matter of fact, the lowest HLR of $0.296 \text{ m}^3/\text{m}^2\cdot\text{h}$ was proven to approach a plug flow reactor with MDI of 1.7, which is below the minimum value of 2 recommended by the EPA. Moreover, this HLR is below what is suggested in the literature, which is $0.7 \text{ m}^3/\text{m}^2\cdot\text{h}$. Consequently, a cost analysis is necessary since a lower HLR may enhance the efficiency of the anaerobic reactor in terms of methane productivity. Additionally, lower HLRs would reduce the need for recirculation pumping, thus contributing to improve the energy efficiency of UASB reactors. To summarize, low HLR applied to the UASB reactor turned out to approach plug flow conditions without observed short circuiting, thus $0.296 \text{ m}^3/\text{m}^2\cdot\text{h}$ is chosen to design such reactor. On the other hand, low HLRs applied to the fixed-film and hybrid reactors resulted in observed short circuiting and no notable differences were observed on the MDI at high HLRs, thus these reactors are designed at $10.632 \text{ m}^3/\text{m}^2\cdot\text{h}$ and $12.450 \text{ m}^3/\text{m}^2\cdot\text{h}$, respectively. Simultaneous inoculation of sludge and plastic media prior to their transfer to UASB, fixed-film, and hybrid reactors was proven to be feasible in this research. Because different approaches are recommended for UASB and fixed-films reactors, they were integrated in this research by switching from steady organic loading rates, recommended for fixed-film reactors, to gradually increasing the OLR by supplying more manure leachate. As a matter of fact, the HRT is recommended to be reduced in order to increase the OLR in UASB inoculations; however, a

steady flow rate was maintained in the system as it is recommended for fixed-film reactors. Nevertheless, the simultaneous inoculation of sludge and plastic media was successfully achieved by obtaining an average percentage of methane of 63% in the inoculation reactor. Moreover, when a sample of plastic media was taken from the inoculation reactor after 18 days to carry out a biochemical methane potential assay, the percentage of methane from three samples were 63%, 63%, and 56% for concentrations of glucose of 0.5, 1, and 2 g/L, respectively. Additionally, the cumulative biogas of the highest concentration behaved as an easily degradable substrate whereas the lower concentration were observed to behave as slowly degradable substrate, which may be attributable to the presence of manure leachate. Upon the transfer of the inoculated sludge to the UASB reactor and bottom section of the hybrid reactor, and the inoculated plastic media to the fixed-film reactor and upper section of the hybrid reactor, the hybrid reactor reached the lowest redox potential before the other two reactors the lowest. Upflow packed-bed reactors (PFR) and hybrid reactors were proven to be suitable to treat manure leachate since the inoculation reactor depicted no inhibition issues at OLR of $4 \text{ kg/m}^3\text{-d}$. On the other hand, when the inoculum was transferred to the high-rate reactors, the experiment was not successfully accomplish since laminar flows were not maintain at the reactors outlets unlike the inoculation reactor. As a result, the developed turbulent flow at such reactors outlets might have disrupted the optimal conditions required by the biomass and intruded air inflow to the system. Thus, an open-channel system at the outlets should be built in future research to guarantee Reynolds numbers below 2000, which are required to achieve laminar flows and maintain high-density biomass inside the high-rate anaerobic reactors.

Last, since a hybrid anaerobic reactor inoculated with biomass obtained from an UASB reactor, plastic media, and manure leachate was successfully operated at an OLR of $4 \text{ kg/m}^3\text{-d}$, the design

criteria and required amendments for high-rate anaerobic reactors a provided for future research. The design judgments are established for the reactors configurations of this research including UASB, fixed-film, and hybrid reactors. Also, these judgments are stated at an average COD concentrations of manure leachate of 26.6 kg/m^3 . Thus, the UASB reactor will be fed with 44 or 88 L/d of manure leachate at OLRs of 15 or $30 \text{ kg/m}^3\text{-d}$, respectively. The fixed-film reactor will be supplied with 15.4 or 51.2 L/d of manure leachate at OLRs of 6 or $20 \text{ kg/m}^3\text{-d}$, respectively. Whereas the hybrid reactor will be fed with 16.9 L/d of manure leachate and an OLR of $6 \text{ kg/m}^3\text{-d}$. With regards to the recycle ratios, the UASB reactor, which will be designed at a low HLR, will required a recycle ratio ranged from 0.15 to 0.06. On the other hand, the fixed-film and hybrid reactors, which will be design at high HLRs, will required recycle ratios ranging from 6 to 20 for the fixed film and 21 for the hybrid reactor. To accomplish the stated HLRs and recycle ratios, it has been recommended for future research to provide individual pumps for feeding and flow recycling, respectively. Moreover, amendments at the inlet and outlet of the high-rate reactors such as manifolds and open-channel flows configurations have been recommended to improve hydrodynamics, keep laminar flows, and avoid air intrusion in the system, thus the most suitable conditions for anaerobic conditions can be maintained for digestion of manure leachate.

REFERENCES

- ANSYS, I. 2011a. ANSYS CFX Introduction. Canonsburg, PA.
- ANSYS, I. 2011b. ANSYS FLUENT User's Guide. Canonsburg, PA.
- ANSYS, I. 2011c. Introduction to ANSYS Meshing. Canonsburg, PA.
- Barker, D.J., Stuckey, D.C. 2001. Modeling of Soluble Microbial Products in Anaerobic Digestion: The Effect of Feed Strength and Composition. *Water Environment Research*, **73**(2), 173-184.
- Cao, X.-c., Zhang, T.-a., Zhao, Q.-y. 2009. Computational simulation of fluid dynamics in a tubular stirred reactor. *Transactions of Nonferrous Metals Society of China*, **19**(2), 489-495.
- Çengel, Y.A., Cimbala, J.M. 2010. *Fluid mechanics : fundamentals and applications*. McGraw-Hill Higher Education, Boston.
- Cresson, R., Escudie, R., Carrere, H., Delgenes, J.P., Bernet, N. 2007. Influence of hydrodynamic conditions on the start-up of methanogenic inverse turbulent bed reactors. *Water Res*, **41**(3), 603-12.
- Deublein, D. 2008. *Biogas from waste and renewable resources an introduction*. Wiley-VCH, Weinheim.
- Deublein, D. 2012. Personal communication.
- Edzwald, J.K. 2011. *Water quality & treatment a handbook on drinking water*. McGraw-Hill, New York.
- Escudie, R., Cresson, R., Delgenes, J.P., Bernet, N. 2011. Control of start-up and operation of anaerobic biofilm reactors: an overview of 15 years of research. *Water Res*, **45**(1), 1-10.
- Griffin, L.P. 2012. Anaerobic Digestion of Organic Wastes: The Impact of Operating Conditions on Hydrolysis Efficiency and Microbial Community Composition. in: *Civil & Environmental Engineering*, Vol. MS, Colorado State University.
- James, A., Chernicharo, C.A.L., Campos, C.M.M. 1990. The development of a new methodology for the assessment of specific methanogenic activity. *Water Research*, **24**(7), 813-825.
- Labatut, R.A., Angenent, L.T., Scott, N.R. 2011. Biochemical methane potential and biodegradability of complex organic substrates. *Bioresour Technol*, **102**(3), 2255-64.
- Lawrence, A.W., McCarty, P.L. 1969. Kinetics of Methane Fermentation in Anaerobic Treatment. *Water Pollution Control Federation*, **41**(2), 1-17.
- Lettinga, G. 1991. UASB-process design for various types of wastewaters. *Water science and technology*, **24**(8), 87-107.
- Manni, G. 1995. Calibration and determination of volatile fatty acids in waste leachates by gas chromatography. *Journal of chromatography. Biomedical applications*, **690**(2), 237-242.
- McCarty, P.L. 1964a. Anaerobic Waste Treatment Fundamentals, Part I, Chemistry and Microbiology. *Public Works 95(September)*, 107-112.
- McCarty, P.L. 1964b. Anaerobic Waste Treatment Fundamentals, Part II, Environmental Requirements and Control. *Public Works 95(October)*, 123-126.
- McCarty, P.L. 1964c. Anaerobic Waste Treatment Fundamentals, Part III, Toxic Materials and Their Control. *Public Works 95(November)*, 91-94.
- Méndez-Romero, D.C., López-López, A., Vallejo-Rodríguez, R., León-Becerril, E. 2011. Hydrodynamic and kinetic assessment of an anaerobic fixed-bed reactor for

- slaughterhouse wastewater treatment. *Chemical Engineering and Processing: Process Intensification*, **50**(3), 273-280.
- Meroney, R.N., Colorado, P.E. 2009. CFD simulation of mechanical draft tube mixing in anaerobic digester tanks. *Water Res*, **43**(4), 1040-50.
- Myint, M.T., Nirmalakhandan, N. 2009. Enhancing anaerobic hydrolysis of cattle manure in leachbed reactors. *Bioresour Technol*, **100**(4), 1695-9.
- Najafpour, G.D., Zinatizadeh, A.A.L., Mohamed, A.R., Hasnain Isa, M., Nasrollahzadeh, H. 2006. High-rate anaerobic digestion of palm oil mill effluent in an upflow anaerobic sludge-fixed film bioreactor. *Process Biochemistry*, **41**(2), 370-379.
- O'Rourke, J.T. 1968. Kinetics of anaerobic treatment at reduced temperatures. in: *PhD Thesis University of Stanford, California, USA (1968)*.
- Owen, W.F., Stucke, D.C., Healy, J.B., Young, L.Y., McCarty, P.L. 1979. Bioassay for monitoring biochemical methane potential and anaerobic toxicity. *Water research*, **13**(6), 485-492.
- Perry, R.H. 2008. *Perry's chemical engineers' handbook*. McGraw-Hill, New York.
- Rittmann, B.E., McCarty, P.L. 2001. *Environmental biotechnology principles and applications*. McGraw-Hill, Boston.
- Sawyer, C.N. 2003. *Chemistry for environmental engineering and science*. McGraw-Hill, Boston.
- Sharvelle, S. 2012. Personal communication.
- Show, K.Y., Wang, Y., Foong, S.F., Tay, J.H. 2004. Accelerated start-up and enhanced granulation in upflow anaerobic sludge blanket reactors. *Water Res*, **38**(9), 2292-303.
- Siedlecka, E.M., Kumirska, J. 2012. Personal communication.
- Siedlecka, E.M., Kumirska, J., Ossowski, P., Glamowski, M., Golebiowski, J., Gajdus, Z., Kaczynski, P., Stepnowski. 2008. Determination of volatile fatty acids in environmental aqueous samples. *Polish Journal of Environmental Studies*, **17**(3), 351-356.
- Speece, R.E. 2008. *Anaerobic biotechnology and odor/corrosion control for municipalities and industries*. Archae Press, Nashville, Tenn.
- Speece, R.E. 1983. Anaerobic biotechnology for industrial wastewater treatment. *Environmental science & technology*, **17**(9), 416-427.
- Speece, R.E. 2012. Personal communication.
- Tchobanoglous, G. 2003. *Wastewater engineering treatment and reuse*. McGraw-Hill, Boston.
- Tong, X., Smith, L.H., McCarty, P.L. 1990. Methane fermentation of selected lignocellulosic materials. *Biomass*, **21**(4), 239-255.
- Valcke, D., Verstraete, W. 1983. A practical method to estimate the acetoclastic methanogenic biomass in anaerobic sludges. *Water Pollution Control Federation* **61**(8), 1191-1195.
- Vavilin, V.A., Fernandez, B., Palatsi, J., Flotats, X. 2008. Hydrolysis kinetics in anaerobic degradation of particulate organic material: an overview. *Waste Manag*, **28**(6), 939-51.
- Venayagamoorthy, S.K. 2012. Personal communication.
- Versteeg, H.K. 2007. *An introduction to computational fluid dynamics the finite volume method*. Pearson Education Ltd, Harlow, England ;
- Wang, X., Ding, J., Guo, W.Q., Ren, N.Q. 2010. A hydrodynamics-reaction kinetics coupled model for evaluating bioreactors derived from CFD simulation. *Bioresour Technol*, **101**(24), 9749-57.
- Wu, B. 2012. Advances in the use of CFD to characterize, design and optimize bioenergy systems. *Computers and Electronics in Agriculture*.

**Appendix A: Stock Solution for Preparation of Define Media for Monitoring Biochemical
Methane Potential**

Table A.1 Stock solution for preparation of define media

Solution	Compound	Concentration
		gL^{-1}
S2-250mL	Resazurin	1
S3-250mL	$(\text{NH}_4)_2\text{HPO}_4$	26.7
S4-250mL	$\text{CaCl}_2 \cdot 2\text{H}_2\text{O}$	16.7
	NH_4Cl	26.6
	$\text{MgCl}_2 \cdot 6\text{H}_2\text{O}$	120
	KCl	86.7
	$\text{MnCl}_2 \cdot 4\text{H}_2\text{O}$	1.33
	$\text{CoCl}_2 \cdot 6\text{H}_2\text{O}$	2
	H_3BO_3	0.38
	$\text{CuCl}_2 \cdot 2\text{H}_2\text{O}$	0.18
	$\text{Na}_2\text{MoO}_4 \cdot 2\text{H}_2\text{O}$	0.17
	ZnCl_2	0.14
S5- 25mL	$\text{FeCl}_2 \cdot 4\text{H}_2\text{O}$	370
S6- 25mL	$\text{Na}_2\text{S} \cdot 9\text{H}_2\text{O}$	500
S7- 2000ml	Biotin	0.002
	Folic acid	0.002
	Pyridoxine hydrochloride	0.01
	Riboflavin	0.005
	Thiamin	0.005
	Nicotinic acid	0.005
	Pantothenic acid	0.005
	B_{12}	0.0001
	p-aminobenzoic acid	0.005
	Thioctic acid	0.005

Appendix B: Raw data of the inoculation reactor

Table B.1 Inoculation reactor start-up by glucose and manure leachate

Day	Leachate Reactor			Inoculation Reactor					
	COD (mg/L)	pH	EC (mS)	OLR (g/L-day)	pH	NaOH added (g)	% of CH4	Cumulative Biogas (m³)	pE (mV)
Glucose	17,233	7.16	10.74	1.40	7.98				-270
					7.58				-280
					1.00	7.18	0.97		-210
					2.00		0.51	67%	-215
					2.00	6.80	2.18		-188
					6.88	5.17			-210
Glucose	46,733	6.26	21.00	2.00	7.32				-230
					7.18	5.00			-250
					7.18	10.78	67%	0.13	-250
					7.24	10.11	79%	0.14	-284
					7.29	11.51	71%	0.15	-267
					7.32	14.21	82%	0.16	-272
Glucose	44,000	6.28	49.10	4.00	7.37	18.46	69%	0.17	-290
					7.46	16.12	82%	0.18	-300
					7.55	18.17	83%	0.19	-306
					7.68	10.05		0.20	-308
					7.74	14.99	54%	0.21	-311
					7.58	10.02		0.22	-315
10	6.32	33.70			8.78	10.07		0.23	-317
11	7.57	29.50			7.62	10.03		0.24	-318
12	6.38	34.80			7.67	20.23		0.25	-319
13	7,200	6.44	35.60		7.77	0		0.26	-322
14	6.68	22.00			7.69	0		0.27	-322
15	6.49	25.60			7.67	0		0.28	-322
16	19,500	6.54	24.00		7.57	0		0.29	-318
18	45,133	6.49	24.60	4	7.58	0	53%	0.30	-316
19	6.61	25.60			7.58	0	78%	0.30	-316
21	6.88	23.90			7.58	0	45%		-316
22	7.07	23.20			7.50	0	61%	0.32	-317
23	6.98	25.60			7.46	0	61%	0.33	-318
25	7.12	23.40			7.44	0	69%	0.34	-319
29	11,700	7.37	24.50		7.40	20.16	78%	0.35	-316
33	21,133	7.48	25.30		7.57	0	61%	0.36	-322
									15.4